Cell Reports

Article

DSB repair pathway choice is regulated by recruitment of 53BP1 through cell cycle-dependent regulation of Sp1

Graphical abstract

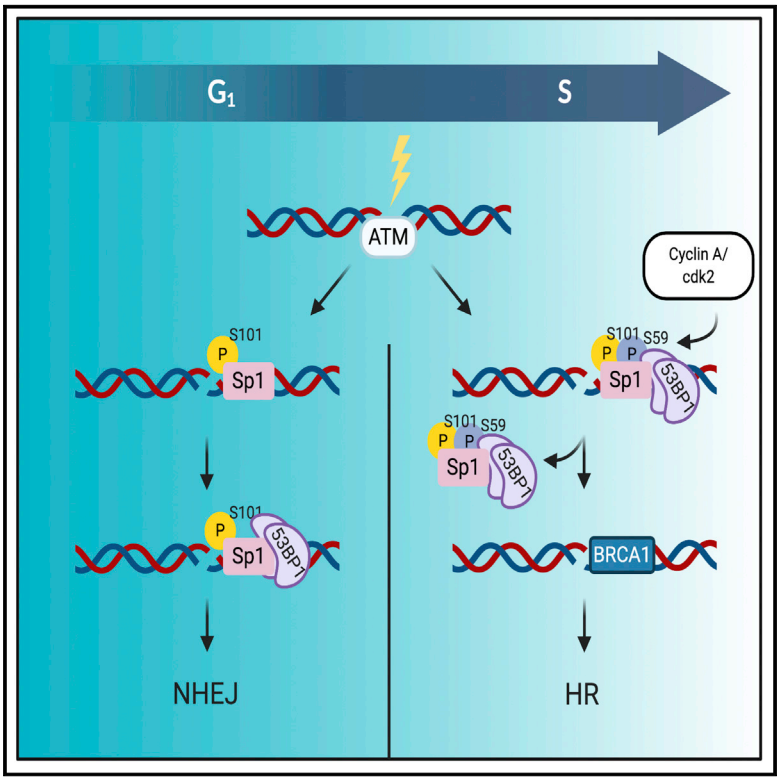

Highlights

- Sp1 is necessary for the recruitment of 53BP1 for the repair of DSBs via NHEJ
- Phosphorylation of Sp1 at the G1/S boundary evicts Sp1 and 53BP1 from DSBs
- Failure to evict Sp1 in S phase perturbs BRCA1 binding, resulting in PARPi sensitivity

Authors

Michelle L. Swift, Kate Beishline, Samuel Flashner, Jane Azizkhan-Clifford

Correspondence

jane.clifford@drexel.edu

In brief

Swift et al. show that Sp1 is necessary for the recruitment of 53BP1 and DSB repair via NHEJ. Phosphorylation of Sp1 by cyclinA/cdk2 at the G1/S boundary evicts Sp1 and 53BP1 from DSBs in S phase, permitting BRCA1 binding. Failure to evict Sp1 in S phase results in PARPi sensitivity.

Swift et al., 2021, Cell Reports *34*, 108840
March 16, 2021
https://doi.org/10.1016/j.celrep.2021.108840

CellPress

Cell Reports

CellPress
OPEN ACCESS

Article

DSB repair pathway choice is regulated by recruitment of 53BP1 through cell cycle-dependent regulation of Sp1

Michelle L. Swift,[1] Kate Beishline,[1,2] Samuel Flashner,[1] and Jane Azizkhan-Clifford[1,3,*]
[1]Department of Biochemistry and Molecular Biology, Drexel University College of Medicine, Philadelphia, PA, USA
[2]Present address: Department of Biological and Allied Health Sciences, Bloomsburg University, Bloomsburg, PA, USA
[3]Lead contact
*Correspondence: jane.clifford@drexel.edu
https://doi.org/10.1016/j.celrep.2021.108840

SUMMARY

Although many of the factors, epigenetic changes, and cell cycle stages that distinguish repair of double-strand breaks (DSBs) by homologous recombination (HR) from non-homologous end joining (NHEJ) are known, the underlying mechanisms that determine pathway choice are incompletely understood. Previously, we found that the transcription factor Sp1 is recruited to DSBs and is necessary for repair. Here, we demonstrate that Sp1 localizes to DSBs in G1 and is necessary for recruitment of the NHEJ repair factor, 53BP1. Phosphorylation of Sp1-S59 in early S phase evicts Sp1 and 53BP1 from the break site; inhibition of that phosphorylation results in 53BP1 and Sp1 remaining at DSBs in S phase cells, precluding BRCA1 binding and suppressing HR. Expression of Sp1-S59A increases sensitivity of BRCA1$^{+/+}$ cells to poly (ADP-ribose) polymerase (PARP) inhibition similar to BRCA1 deficiency. These data demonstrate how Sp1 integrates the cell cycle and DSB repair pathway choice to favor NHEJ.

INTRODUCTION

Double-strand breaks (DSBs) are the most threatening type of DNA damage and are repaired by two major DNA repair pathways: non-homologous end joining (NHEJ) and homologous recombination (HR). DSB repair is tightly interwoven with cell cycle progression because cell cycle phase is one of the main determinants of DSB repair pathway choice. 53BP1 and BRCA1 are recruited to DSBs to facilitate NHEJ or HR, respectively (Bensimon et al., 2010; Her and Bunting, 2018). 53BP1 is an adaptor/mediator protein that serves as a platform for recruitment of other repair factors and blocks end resection in G1, thereby operating as a key positive regulator of NHEJ (Bouwman et al., 2010). 53BP1 loss rescues BRCA1 deficiency and is associated with triple-negative and BRCA1-mutated breast cancers (Chapman et al., 2013; Schultz et al., 2000). 53BP1 is an early participant in the cellular response to DSBs (Schultz et al., 2000; Xia et al., 2001). In the S phase, 53BP1 is evicted from the break site to allow BRCA1 binding and the subsequent resection of the 5′ end of the DSB to initiate invasion into the homologous strand for HR (Feng et al., 2015; Nacson et al., 2018). Regulation of hand off between 53BP1 and BRCA1 at DSBs is not well understood. Here, we identify a molecular switch that activates the removal of 53BP1 and facilitates BRCA1 binding exclusively in S/G2.

Although end resection and proximity to a repair template are important in determining which repair pathway is used for DSB repair, it is also known that different cell types use one repair pathway more frequently than the other. Highly proliferative cells, such as stem cells, preferentially use HR. Meanwhile more-differentiated cell lines and post-mitotic cells use NHEJ (Mujoo et al., 2017), Therefore, DSB repair pathway choice must be highly regulated at many different stages. One of the main determinants of DSB repair pathway choice is the cell cycle phase. HR reaches peak activity in the mid-S phase, whereas NHEJ predominates in G1 (Karanam et al., 2012). The interdependence of the DSB repair pathways and the cell cycle is controlled by a number of factors, including cyclins and cyclin-dependent kinases (CDKs) (Agami and Bernards, 2000; Branzei and Foiani, 2008). Checkpoint signaling activation and CDK-dependent phosphorylation of repair factors regulate repair protein stability, activity, and recruitment. The coordination between cell cycle and DSB repair pathway choice is critical for choosing the appropriate repair pathway in a specific cell cycle phase (Bennett et al., 2013). The signals that integrate cell cycle progression and the DSB repair pathway choice are not entirely understood and constitute an active area of research because dysregulation of these pathways can lead to genomic instability and cell death or cellular transformation.

Among the many proteins involved in recognition of DSBs is specificity protein 1 (Sp1), which has also been implicated in DSB repair (Beishline et al., 2012; Fletcher et al., 2018; Olofsson et al., 2007). Sp1 is ubiquitously expressed and best known as a transcription factor that regulates genes involved in DNA repair, apoptosis, and cell proliferation (Black et al., 2001; Deniaud et al., 2009; Torabi et al., 2018). Sp1's activity is regulated by

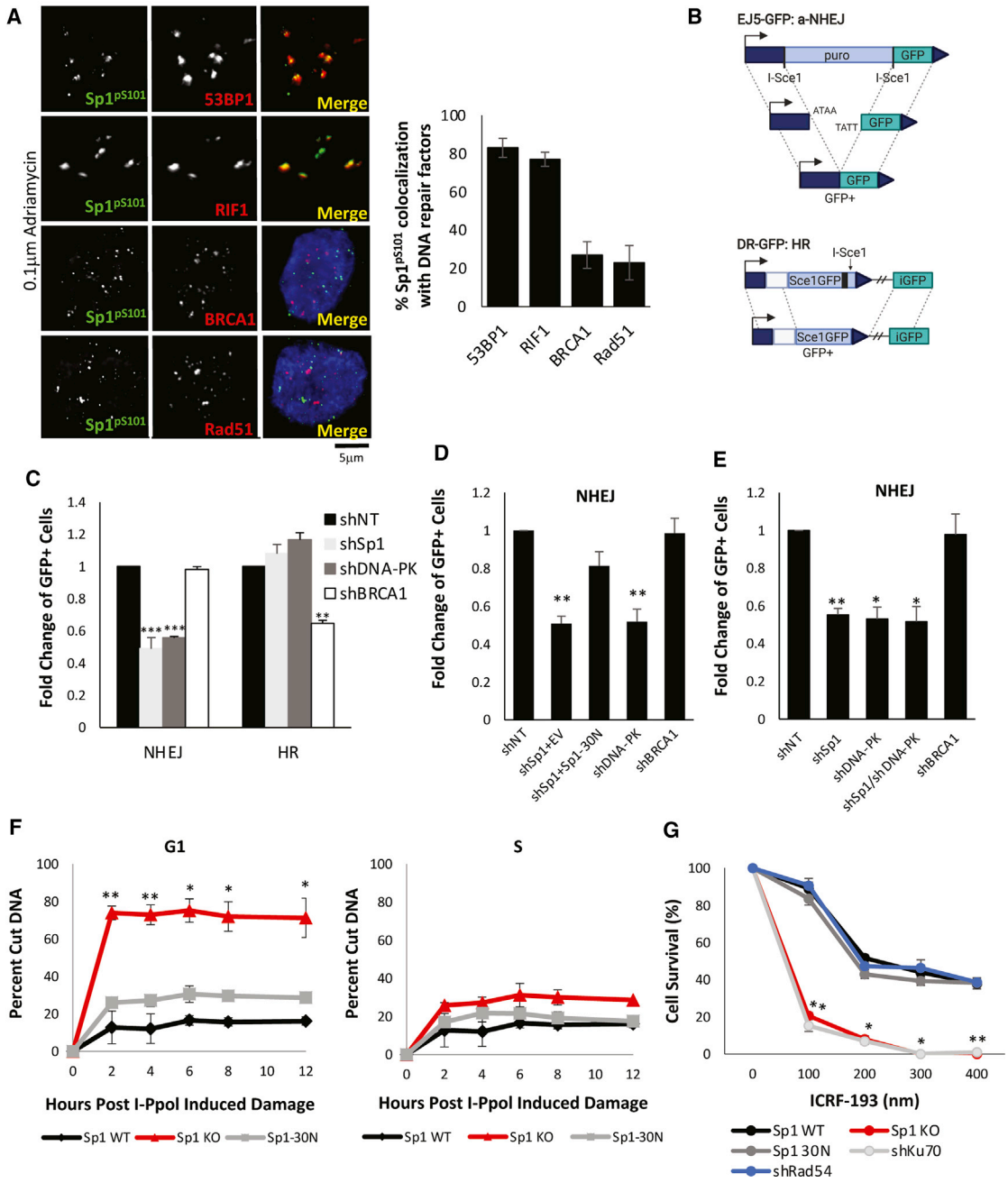

Figure 1. Sp1 colocalizes with NHEJ repair factors and is necessary for repair

(A) U2OS cells were pretreated with 10 mM BrdU for 3 h to label cells in the S phase (blue). Cells were treated with 0.1 μM Adriamycin for 1 h and processed for immunofluorescence using $Sp1^{pS101}$, 53BP1, RIF1, BRCA1, Rad51, or BrdU antibodies.

(B) Schematic of a-NHEJ and HR GFP reporter assays. Created with BioRender.com

(C–E) U2OS cells stably expressing EJ5 (C–E) or DR-GFP (C) reporter constructs expressing non-targeting Sp1, DNA-PK, BRCA1 shRNA (C–E), or shSp1+ empty vector (EV) and shSp1+Sp1-30N (D) were infected with I-Sce1 lentivirus. 72 h after infection, DNA repair was assessed by flow cytometry of GFP^+ cells.

(F) In cells expressing I-PpoI, Sp1 was knocked out using sgRNA targeting Sp1 and either a FLAG-tagged full-length (FL), EV, or FLAG-tagged Sp1-30N mutant was expressed by lentiviral transduction (shown in Figure S1E). Cells were synchronized in the G1or S phase, followed by DSB induction with 4-OHT. DNA was isolated from cell lysates at various time points after induction of I-PpoI, and ChIP was performed with a γH2Ax antibody, followed by qPCR using primers spanning the break site.

(G) Sp1 was knocked out in UWB 1.289 $BRCA1^{+/+}$ cells, and $Sp1^{WT}$, empty vector (Sp1 KO), $Sp1^{30N}$, or shRNA against Ku70 or Rad54 (shown in Figure S1G) were expressed by lentiviral transduction. Cells were seeded in agar and treated with the indicated doses of ICRF-193. Cells were incubated for 14 days, followed by staining and quantification.

(legend continued on next page)

post-translational modifications that modulate its DNA binding, trans-activation activity, stability, and localization (Beishline and Azizkhan-Clifford, 2014; Bouwman and Philipsen, 2002; Fojas de Borja et al., 2001; Wang et al., 2011). In what appears to be a transcription-independent function, Sp1 is phosphorylated on serine 101 ($Sp1^{pS101}$) by DNA damage response factor ataxia telangiectasia mutated (ATM) (Olofsson et al., 2007) in response to induction of DSBs. $Sp1^{pS101}$ localizes to DSBs, along with the phosphorylated histone variant H2Ax (γH2Ax) and the MRN complex member, Nbs1, which likely promotes its recruitment to DSBs (Beishline et al., 2012). Sp1 is important for repair of DSBs because loss of Sp1 results in defective DSB repair (Beishline et al., 2012). The repair defect resulting from Sp1 depletion can be rescued by expression of the N-terminal 182 aa portion of Sp1, which localizes to DSBs, is phosphorylated by ATM on S101, and lacks the zinc finger sequence-specific DNA binding region (Beishline et al., 2012). Therefore, Sp1's role in DNA damage recognition and repair is independent of its classic transcriptional activity. However, this new role for Sp1 in DSB repair has, thus far, remained mechanistically undefined.

The studies herein demonstrate that Sp1 selectively promotes repair of DNA DSBs by NHEJ through its phosphorylation by cyclin A/cdk2 site (Banchio et al., 2004; Fojas de Borja et al., 2001) ($Sp1^{pS59}$) in the early S phase. The phosphorylation controls its association with DSBs and acts as a cell cycle sensor to control initiation of NHEJ or HR. The absence of phosphorylation at this site generates defects in BRCA1 recruitment and HR and sensitizes $BRCA^{+/+}$ cells to poly (ADP-ribose) polymerase (PARP) inhibition. Here, we describe the mechanism by which Sp1 promotes DNA repair and identify cdk2 phosphorylation of Sp1 as a molecular switch that controls the transition from NHEJ to HR in the early S phase.

RESULTS

Sp1 colocalizes with NHEJ repair factors and is necessary for NHEJ repair

We have previously shown that Sp1 is phosphorylated by ATM in response to DSBs (Olofsson et al., 2007). Sp1 phosphorylated on serine 101 ($Sp1^{pS101}$) co-localizes with γH2AX at DSBs and is necessary for proper repair. Sp1's role appears to be independent of its effect on transcription because expression of the N-terminal 182 aa Sp1 peptide (Sp1-30N), which lacks its zinc finger DNA-binding domain, can still localize to DSBs and promote repair (Beishline et al., 2012). To further characterize Sp1's role in DSB repair, we sought to determine the DSB repair pathway in which Sp1 is involved.

Using immunofluorescence (IF), we determined that $Sp1^{pS101}$ forms discrete foci that colocalize with NHEJ repair factors 53BP1 and RIF1 in response to damage induced by Adriamycin in U2OS and hTert RPE-1 cells (Figures 1A and S1A). γH2AX, a histone variant that is phosphorylated on S139 near DSBs, is also localized to these foci. In these same cells, $Sp1^{pS101}$ fails to colocalize with the HR repair factors BRCA1 and Rad51 (Figures 1A and S1A). Together, these data suggest that Sp1 may be functioning in NHEJ and not HR. To validate Sp1's role in NHEJ, we used two different GFP reporter assays to measure DSB repair by classical NHEJ (c-NHEJ), alternative NHEJ (a-NHEJ), and HR (DR-GFP) (Bennardo et al., 2008). The defective GFP genes each contain an I-Sce1 endonuclease site at which a single-site-specific DSB is induced by I-Sce1; correct repair of those DSBs by their respective pathway results in a functional GFP gene, the activity of which can be measured using flow cytometry (Figure 1B) (Liu et al., 2013). U2OS cells expressing the a-NHEJ GFP reporter (Bennardo et al., 2008; Qi et al., 2016) and depleted of Sp1 show a reduction in NHEJ comparable to knockdown of the NHEJ repair factor DNA-PK (Figures 1C and S1B). Conversely, knockdown of HR-specific factor BRCA1 had no effect on NHEJ. Knockdown of Sp1 in U2OS cells expressing the HR GFP reporter (DR-GFP) did not significantly affect HR, as measured by GFP expression, whereas BRCA1 knockdown significantly reduced HR (Figures 1C and S1B). To confirm that this observation was independent of Sp1's role in transcriptional regulation, we evaluated whether expression of Sp1-30N was sufficient to restore NHEJ in Sp1-knockdown cells. Consistent with our previous results, Sp1-30N can rescue the repair defect induced by Sp1 knockdown, and that defect is in NHEJ (Figures 1D and S1C) (Beishline et al., 2012). Furthermore, knockdown of both Sp1 and DNA-PK did not further reduce NHEJ compared with knockdown of each factor alone (Figures 1E and S1D), indicating that these two factors likely function in the same pathway. Because the a-NHEJ reporter assay does not directly measure the repair efficiency of cells undergoing classical NHEJ alone, those experiments were repeated using a third GFP reporter assay, EJ7 c-NHEJ, (Bhargava et al., 2018). $Sp1^{-/-}$ U2OS cells were transduced with lentivirus containing an empty vector, FLAG-tagged Sp1 wild type (WT) or Sp1-30N driven by the endogenous Sp1 promoter (Figure S1E). After Sp1 knockout by single-guide RNA (sgRNA), we observed a decrease in c-NHEJ repair, similar to that seen with knockout of Ku70. The defect in c-NHEJ in $Sp1^{-/-}$ cells can be rescued by expression of Sp1-30N (Figure S1F). We did not observe any additional effects on c-NHEJ upon depletion of both Sp1 and Ku70 (Figure S1F).

To confirm that Sp1 is functioning to repair DSBs in the G1 phase, as expected for NHEJ, we synchronized cells in the G1 or S phase and measured DSB repair using the endonucleases I-PpoI to induce sequence-specific DSBs at unique genomic locations (Berkovich et al., 2007). Repair of DSBs can be quantified by chromatin immunoprecipitation (ChIP) and qPCR using primer sets flanking the break site. We used that system to assess Sp1's role in DSB repair in the G1 and S phases of the cell cycle. $Sp1^{-/-}$ cells in G1 displayed significant defects in repair, whereas cells arrested in the S phase showed no repair defects (Figures 1F and S1G). Expression of Sp1-30N rescues the G1 repair defect in Sp1 knockout cells (Figure 1F).

Data represent means ± SEM from three independent experiments assessed in triplicate. In (C)–(G), a t test was performed comparing each shRNA to non-targeting shRNA. *$p < 0.05$, **$p < 0.01$, or ***$p < 0.001$. No asterisk (*) indicates $p > 0.05$. Western blots showing knockdown and re-expression are shown in Figure S1.

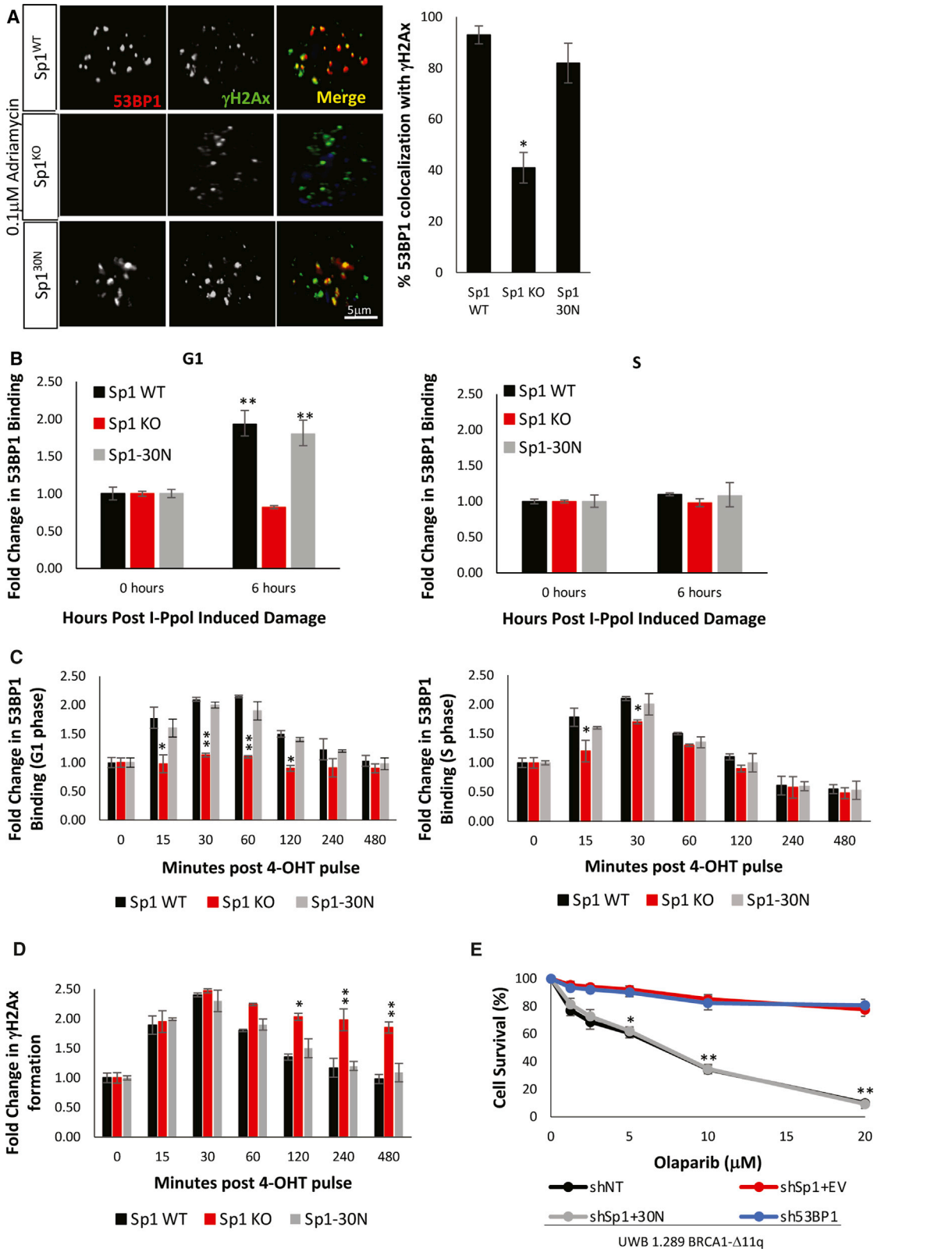

(legend on next page)

Additionally, we confirmed Sp1's role in NHEJ by performing a colony-formation assay in the presence of ICRF-193, a topoisomerase II inhibitor to which cells deficient in NHEJ display increased sensitivity (Adachi et al., 2003, 2004; Maede et al., 2014). Sp1 knockout cells treated with ICRF-193 displayed increased sensitivity relative to control cells, comparable to knockdown of the NHEJ repair factor Ku70 (Figures 1G and S1H). Together, these results indicate that Sp1 is required for repair of DSBs by NHEJ.

Sp1 is necessary for recruitment of 53BP1 to DSBs

To elucidate the mechanism by which Sp1 regulates NHEJ, we first sought to determine whether recruitment of 53BP1, the key-positive regulator of NHEJ, is affected by Sp1 depletion. 53BP1 blocks DNA end resection, which is essential for NHEJ (Bunting et al., 2010; Chapman et al., 2013). We performed immunofluorescence in $Sp1^{-/-}$ cells transduced with an empty vector, FLAG-tagged Sp1 WT or Sp1-30N (Figure S1E), followed by immunofluorescence for 53BP1. As shown in Figure 2A, 53BP1 is not recruited in $Sp1^{-/-}$ cells, but recruitment is rescued by WT Sp1 and by Sp1-30N (Figure 2A). Similarly, colocalization of 53BP1 and γH2Ax foci is reduced in hTert RPE-1 $Sp1^{-/-}$ cells, which can also be rescued upon expression of Sp1-30N (Figure S2A). To further examine 53BP1 recruitment, we transfected the same three cell types with GFP-tagged 53BP1 (Figure S2B) and performed fluorescence recovery after photobleaching (FRAP). Cells were pre-treated with bromodeoxyuridine (BrdU) so that DNA in the region of interest (ROI) undergoes laser-induced DSBs. The recovery of the fluorescence signal is measured as a function of time, and the rate at which the fluorescence recovers provides a measure of the mobility and recruitment of tagged proteins. Cells depleted of Sp1 showed a significant delay in GFP-53BP1 fluorescence recovery to the ROI, which was alleviated upon expression of Sp1-30N (Figures S2C and S2D). To confirm that Sp1 affects 53BP1 binding to DSBs, we used I-PpoI cleavage and 53BP1 ChIP. We observed that Sp1 knockout results in decreased binding of GFP-53BP1 to DSBs specifically in G1, which could be rescued upon expression of Sp1-30N (Figures 2B and S3A). The duration of this defect was quantified using I-PpoI and ChIP, in which we measured 53BP1 recruitment over time in $Sp1^{-/-}$ cells synchronized in the early G1 or early S phase after a 30-min pulse of 4-OHT. $Sp1^{-/-}$ cells displayed decreased recruitment of 53BP1 throughout the G1 phase and early S phase after induction of DSBs (Figure 2C). Furthermore, we observed the prolonged presence of γH2Ax foci at DSB sites in the G1 phase, suggesting that failure to recruit Sp1 and hence 53BP1 results in unresolved damage (Figure 2D). Knockdown of 53BP1 does not affect the recruitment of $Sp1^{pS101}$ to ionizing radiation-induced nuclear foci (IRIFs), suggesting that Sp1 localizes to DSBs independently of 53BP1 and is likely recruited upstream of 53BP1 recruitment (Figure S3B).

Loss of 53BP1 in a BRCA1-null cell restores HR, thereby making cells less sensitive to PARP inhibition (Krais et al., 2020; Nacson et al., 2018; Zong et al., 2019). We hypothesized that if Sp1 is necessary to recruit 53BP1, cells deficient in Sp1 would also be resistant to PARP inhibition. As expected, BRCA1-Δ11q cells with short hairpin RNA (shRNA)-mediated 53BP1 depletion displayed decreased sensitivity to PARP inhibition, and we found that UWB 1.289 BRCA-Δ11q cells expressing shRNA against Sp1 exhibited decreased sensitivity to PARP inhibition, comparable to that observed with 53BP1 knockdown and that the sensitivity was restored by expression of Sp1-30N (Figures 2E and S3C). These data strongly suggest that Sp1 is required for recruitment of 53BP1 and that Sp1-30N is sufficient to mediate this recruitment. The mechanism of recruitment does not appear to be the interaction between Sp1 and 53BP1 because no interaction was detected by co-immunoprecipitation (Figure S3D).

Sp1 acts as a cell cycle sensor to ensure proper repair pathway choice

Cell cycle phase is one of the main determinants of DSB-repair pathway choice. The coordination of the DSB-repair pathway and the cell cycle is controlled through a variety of factors, including CDKs (Agami and Bernards, 2000; Branzei and Foiani, 2008). Activation of checkpoint signaling and CDK-dependent phosphorylation are critical regulators of repair protein stability, activity, and recruitment. That signaling axis is crucial for appropriate repair in a specific cell cycle phase (Bennett et al., 2013). Because of Sp1's role in NHEJ, the repair pathway confined to G1, we evaluated whether Sp1 localization was affected by cell cycle phase. We prelabeled cells with BrdU to identify S phase cells and treated them with Adriamycin. We found that $Sp1^{pS101}$ colocalized with γH2Ax only in the G1 phase cells. (Figure S4A). This led us to further investigate the role of the cell cycle on Sp1's function and regulation in DSB repair. Upon entry into the S phase and activation of cyclin A/cdk2, Sp1 interacts with cyclin A (Figure S4B) and is phosphorylated on serine 59

Figure 2. Sp1 is necessary for 53BP1 recruitment to DSBs

(A) U2OS cells expressing sgRNA against Sp1 and re-expressing FLAG-full-length Sp1, EV, or FLAG-Sp1-30N were pretreated with 10 μM BrdU for 3 h to label cells in the S phase (blue). Cells were treated with 0.1 μM Adriamycin for 1 h and processed for immunofluorescence using 53BP1 and γH2Ax antibodies.

(B–D) In cells expressing I-PpoI, Sp1 was knocked out using sgRNA targeting Sp1 and either a FLAG-tagged full-length Sp1-WT, EV, or FLAG-tagged Sp1-30N mutant was expressed by lentiviral transduction, followed by transfection with GFP-53BP1.

(B) Cells were synchronized in the G1 or S phase, followed by DSB induction with 4-OHT.

(C and D) Cells were synchronized in G1 (2C, left, and 2D) or S (2C, right) phase followed by induction DSB induction with 4-OHT. 4-OHT was removed after 30 min.

(B–D) DNA was isolated from cell lysates at various time points after induction of I-PpoI, and ChIP was performed using a GFP or γH2Ax antibody, followed by qPCR using primers spanning the break site.

(E) Sp1 was knocked down in UWB 1.289 BRCA1-Δ11q and EV or Sp1-30N was expressed by lentiviral transduction. Non-targeting and 53BP1 shRNA were also expressed via lentiviral transduction (shown in Figure S3C). Cells were seeded in agar and treated with indicated doses of olaparib. Cells were incubated for 14 days followed by staining and quantification.

Data represent means from three independent experiments assessed from 30 cells per experiment. For (A)–(D), statistical analysis was performed as in Figure 1.

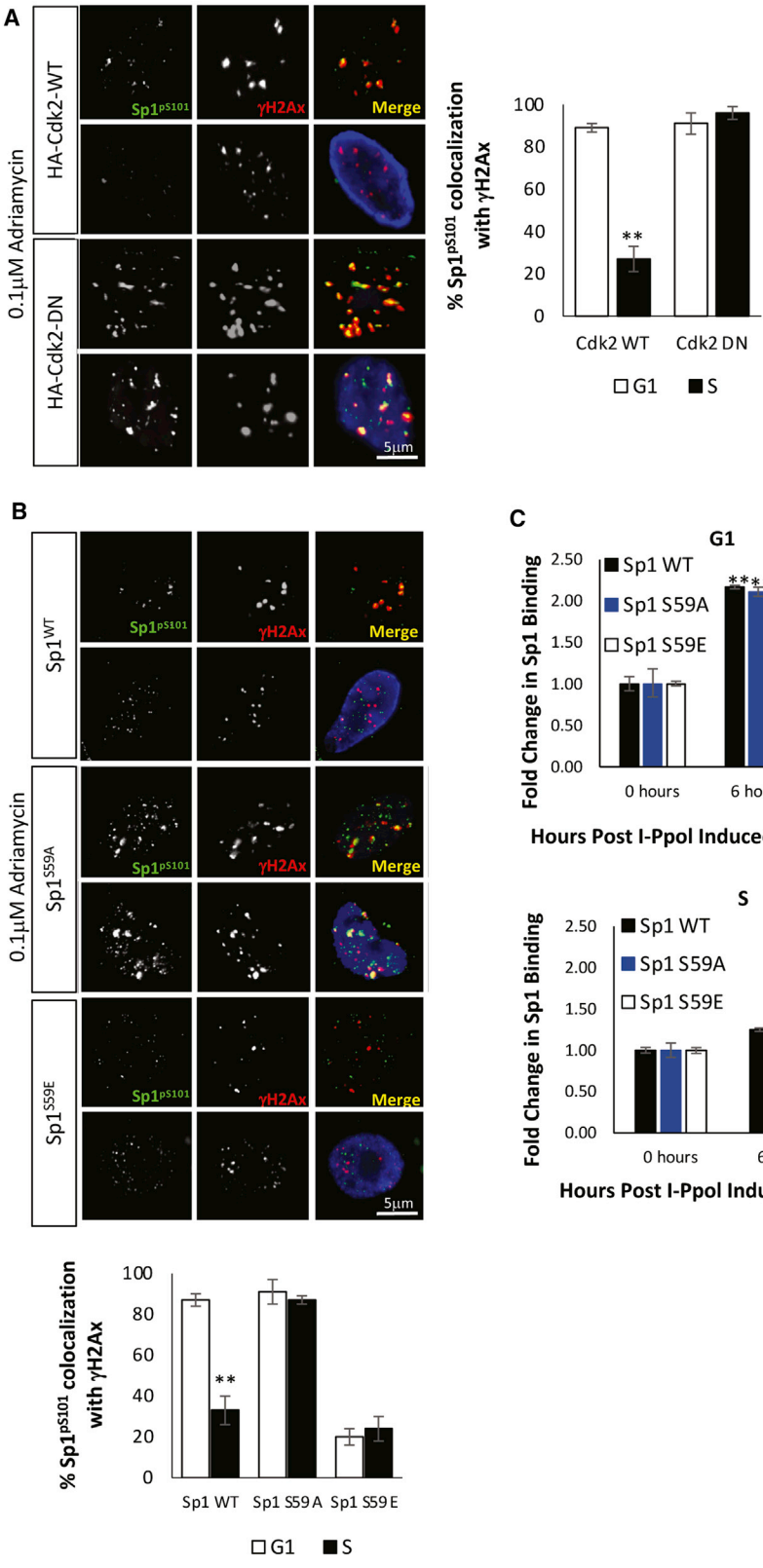

(legend on next page)

(Banchio et al., 2004; Fojas de Borja et al., 2001; Kang et al., 2012; Kim and Lim, 2009; Spengler et al., 2008). We overexpressed either a WT Cdk2 or dominant-negative Cdk2 (Figure S4C) and evaluated the role of cyclin A/cdk2 in $Sp1^{pS101}$ localization in the G1 and S phase cells. In cells expressing WT cdk2, we observed colocalization of $Sp1^{pS101}$ with γH2Ax in the G1 phase only, whereas in cells expressing dominant-negative Cdk2, we observed colocalization between $Sp1^{pS101}$ and γH2Ax in both G1 and S phase cells (Figure 3A). Together, these data suggest that phosphorylation by cyclin A/cdk2 regulates localization of $Sp1^{pS101}$ at DSBs. We next expressed FLAG-tagged WT Sp1, cyclin A/cdk2 phospho-null mutant ($Sp1^{S59A}$), or cyclin A/cdk2 phosphomimetic mutant ($Sp1^{S59E}$) in U2OS $Sp1^{-/-}$ cells (Figure S1E). Similar to WT Sp1, $Sp1^{S59A}$ was phosphorylated at serine 101 in response to damage and colocalized with γH2Ax in G1 cells; however, unlike WT Sp1, $Sp1^{S59A}$ also colocalized with γH2Ax in S phase cells (Figure 3B). Moreover, in cells expressing $Sp1^{S59E}$, we observed no colocalization between $Sp1^{pS101}$ and γH2Ax in either G1 or S phase cells (Figure 3B). We next used I-PpoI/ChIP to confirm that $Sp1^{WT}$ is recruited to DSBs in cells synchronized in G1 but not in cells allowed to progress into the S phase (Figure S5A). We found that $Sp1^{S59A}$ is present at DSBs in both the G1 and S phase, whereas $Sp1^{S59E}$ is not present at DSBs in either the G1 or the S phase (Figure 3C).

We further investigated the effects of cyclin A/cdk2 phosphorylation of Sp1 on DNA repair using the I-PpoI repair assay. Cells expressing $Sp1^{S59E}$ have defective DNA repair in G1, whereas cells expressing $Sp1^{S59A}$ show repair defects in S phase (Figures 4A and S5A). To confirm that these results were representative of either NHEJ or HR repair, we used the two GFP reporter assays to measure repair by NHEJ and HR (DR-GFP) (Bennardo et al., 2008; Qi et al., 2016) (Figure S5B). U2OS cells expressing $Sp1^{S59A}$ had NHEJ repair efficiency similar to cells expressing Sp1 WT, whereas cells expressing $Sp1^{S59E}$ (Figure S5C) were defective in both a-NHEJ and c-NHEJ repair (Figure 4B). In contrast, cells expressing $Sp1^{S59A}$ displayed defects in HR, but $Sp1^{S59E}$ cells did not. Additionally, we determined the sensitivity of cells expressing Sp1-cyclin A/cdk2 mutant (Figure S5D) to treatment with the topoisomerase II inhibitor, ICRF-193. In contrast to cells expressing shRNA against the HR repair protein Rad54, cells expressing $Sp1^{S59E}$ showed increased sensitivity to ICRF-193, similar to knockdown of 53BP1 (Figure 4C). In a third independent NHEJ assay, telomere end joining (Smogorzewska and de Lange, 2002), $Sp1^{S59E}$ cells showed defects in NHEJ similar to Sp1 knockout and 53BP1 knockdown (Figures 4D and S5E). These data strongly indicate that cell cycle regulation of Sp1 via phosphorylation of $Sp1^{S59}$ by cyclin A/cdk2 regulates Sp1 recruitment to and retention at the break site to regulate DSB repair pathway choice.

To determine whether these repair defects associated with S59 phosphorylation were due to aberrant recruitment of 53BP1 to DSBs by Sp1, we evaluated 53BP1 recruitment to DSBs via FRAP in the Sp1-S59 phospho mutants (Figure S6A). The $Sp1^{S59E}$ mutants had delayed GFP-53BP1 recovery after bleaching (Figures S6B and S6C), consistent with the observed repair defect. We then sought to determine whether these mutants displayed changes in repair factor recruitment to DSBs in the G1 and S phases (Figure S6D). Similar to WT cells, 53BP1 and γH2Ax colocalized in the G1 cells expressing $Sp1^{S59A}$; moreover, this colocalization persisted in the S phase. In contrast, 53BP1 and γH2Ax failed to colocalize in both cell cycle phases in $Sp1^{S59E}$ cells, which do not retain Sp1 at the break site in G1 or S. This suggests that retention of Sp1 at DSBs is critically important to maintain 53BP1 binding (Figure 5A, left). We next assessed whether Sp1 at DSBs in S phase perturbs HR repair factor recruitment. $Sp1^{S59A}$ cells have decreased colocalization of BRCA1 to γH2Ax foci in S phase compared with WT Sp1 cells. Additionally, in cells expressing $Sp1^{S59E}$, the BRCA1 recruitment defect in S phase cells is rescued, and no recruitment of BRCA1 was seen in G1 cells (Figure 5A, right). This is consistent with the report that BRCA1 is degraded in G1 to prevent aberrant recruitment (Baer and Ludwig, 2002; Wu-Baer et al., 2003). To further validate these results, we used I-PpoI/ChIP to assess 53BP1 and BRCA1 recruitment to DSBs upon expression of the Sp1-cyclin A/cdk2 phospho mutants. In cells expressing $Sp1^{S59A}$, 53BP1 is not only recruited in the G1 phase, similar to WT cells, but also in the S phase. Alternatively, in cells expressing $Sp1^{S59E}$ (Figure S6E), 53BP1 is not recruited in the G1 or the S phase (Figure 5B). $Sp1^{S59A}$ inhibits BRCA1 recruitment in the S phase, whereas BRCA1 recruitment is not affected in WT or $Sp1^{S59E}$-expressing cells (Figures 5C and S6F). These data suggest that Sp1 is recruited to DSBs in G1 to recruit 53BP1 and is removed in S phase for 53BP1 eviction to allow BRCA1 binding.

To further characterize the effects of inappropriate retention or eviction of Sp1 on 53BP1 recruitment and DSB repair, we examined the effect of expression of Sp1-cyclin A/cdk2 phospho mutants on formation of Rad51 foci in a BRCA1-mutated cell line, UWB 1.289 BRCA1-Δ11q cells. Cells harboring the mutated BRCA1-Δ11q splice isoform, which are also deficient in 53BP1 recruitment, are able to activate proteins downstream of end resection to promote Rad51 loading and HR (Nacson et al., 2018; Zong et al., 2019). Because $Sp1^{-/-}$ cells and cells expressing $Sp1^{S59E}$ fail to recruit 53BP1, we assessed whether

Figure 3. Cyclin A/cdk2-depedent phosphorylation of Sp1 removes Sp1 from DSBs

(A) U2OS cells were transfected with Cdk2 WT or a Cdk2-dominant negative; 72 h after transfection, cells were prelabeled with BrdU for 3 h. Cells were subjected to 0.1 μM Adriamycin for 1 h, fixed, and processed for immunofluorescence using $Sp1^{pS101}$, γH2Ax, and BrdU antibodies.

(B and C) Sp1 was knocked out using sgRNA targeting Sp1 and FLAG-tagged FL $Sp1^{WT}$, EV, $Sp1^{30N}$, and $Sp1^{S59A}$ or $Sp1^{S59E}$ phospho mutants were expressed by lentiviral transduction.

(B) U2OS cells described above were prelabeled for 3 h with 10 μM BrdU. Cells were then subjected to 0.1 μM Adriamycin for 1 h, fixed, and processed for immunofluorescence using $Sp1^{pS101}$, γH2Ax, and BrdU antibodies.

(C) U2OS cells expressing I-PpoI described above were synchronized in the G1 or S phase and treated with 4-OHT to induce DSBs. DNA was isolated from cell lysates 6 h after induction of I-PpoI, and ChIP was performed using a FLAG antibody, followed by qPCR using primers in close proximity to the break site. Data represent means ± SEM from three independent experiments done in triplicate. Statistical analysis was performed as in Figure 1.

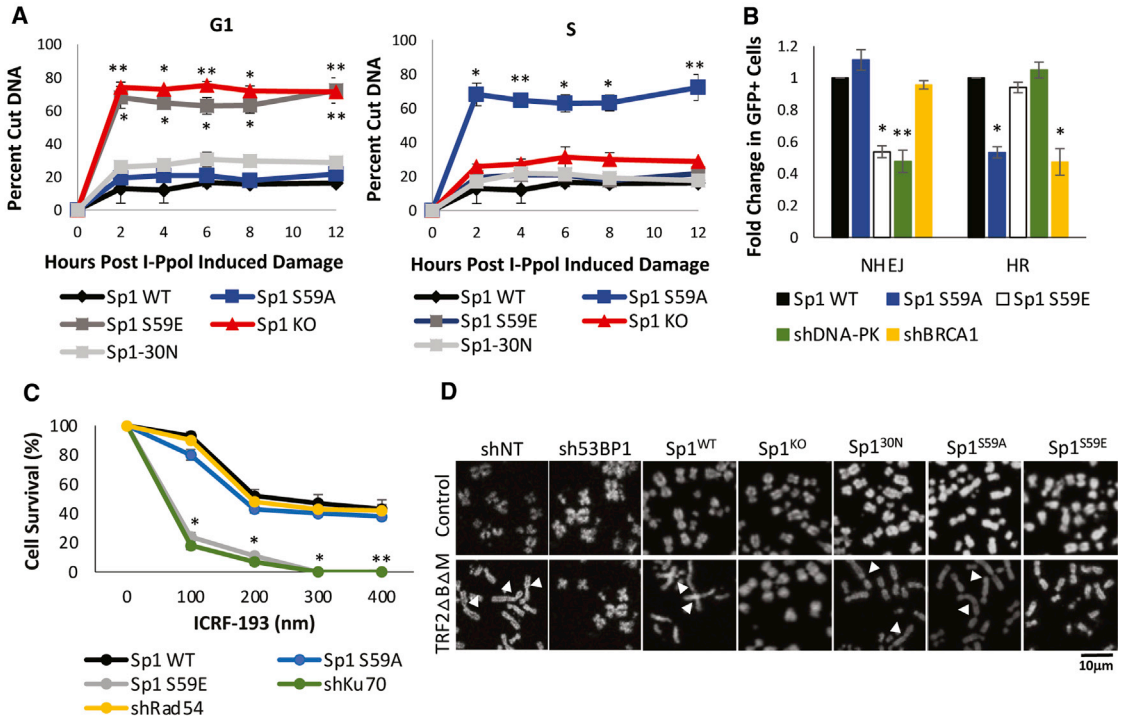

Figure 4. Cyclin A/cdk2-depedent phosphorylation of Sp1 affects DSB repair efficiency

(A–D) Sp1 was knocked out using sgRNA targeting Sp1 and FLAG-tagged FL Sp1^{WT}, EV, Sp1^{30N}, and Sp1^{S59A} or Sp1^{S59E} phospho mutants were expressed by lentiviral transduction.

(A) U2OS cells expressing I-PpoI described above were synchronized in the G1 or S phase and treated with 4-OHT to induce DSBs. DNA was isolated from cell lysates at various time points after induction of I-PpoI, and ChIP was performed using a γH2Ax antibody, followed by qPCR using primers flanking the break site.

(B) Sp1 was knocked out by CRISPR-Cas9 in U2OS cells stably expressing EJ5 or DR-GFP reporter constructs. Cells were transduced with vectors encoding Sp1 WT, S59A, and S59E or shRNA targeting DNA-PK or BRCA1. Cells were infected with I-Sce1 lentivirus, and 72 h after infection, DNA repair was assessed by flow cytometry of GFP^{+} cells.

(C) Sp1 was knocked out in UWB 1.289 BRCA1$^{+/+}$ cells, and Sp1^{WT}, Sp1S^{59A}, Sp1^{S59E} or shRNA against Ku70 or Rad54 (shown in Figure S5D) were expressed by lentiviral transduction. Cells were seeded in agar and treated with the indicated doses of ICRF-193. Cells were incubated for 14 days after staining and quantification.

(D) Mitotic spreads of U2OS cells expressing sgRNA against Sp1, then transduced with Sp1^{WT}, EV, Sp1^{30N}, or the Sp1-cyclin A/cdk2 phospho mutants. Sp1^{WT} were additionally transduced with shNT or sh53BP1. All cells were additionally transduced with EV or *N*-Myc-TRF2ΔBΔM to allow for telomere end joining (shown in Figure S5E). DAPI was used to visualize fused chromosomes. Arrows indicate fused telomere ends.

Data in (A)–(C) represent means ± SEM from three independent experiments done in triplicate. Statistical analysis was performed as in Figure 1.

Rad51 foci would form in BRCA1-Δ11q cells. Similar to Sp1$^{-/-}$ cells, Sp1^{S59E} cells display an increase in Rad51 foci per nucleus as well as an increase in the percentage of nuclei with Rad51 foci in the BRCA1-deficient cells (Figure 6A).

We further hypothesized that, because cells expressing Sp1^{S59A} could not recruit BRCA1 in the S phase, these cells would have increased sensitivity to PARP inhibition, similar to BRCA1-deficient cells. We found that UWB 1.289 cells expressing full-length WT BRCA1 and Sp1^{S59A} (Figure S6G) have increased sensitivity to PARP inhibition, comparable to BRCA1-Δ11q cells treated with a PARP inhibitor (Figure 6B).

Together, these data suggest that Sp1 is phosphorylated upon entry into the S phase to remove Sp1 from the break site, allowing BRCA1 to bind and initiate HR. These data support a role for Sp1 as a cell cycle molecular switch to ensure proper repair factor binding and repair pathway choice (Figures 3, 4, 5, and 6).

DISCUSSION

We and others have shown that Sp1 is phosphorylated by ATM and is necessary for repair of DSBs, independent of its role as a transcription factor; however, the mechanism by which Sp1 modulates repair was not previously explored (Beishline et al., 2012; Fletcher et al., 2018; Olofsson et al., 2007). The data presented herein reveal a new mechanism whereby Sp1 can mediate repair pathway choice. Importantly, this article provides further insight into how these repair mechanisms are regulated and how defects in these processes can be exploited in cancer therapeutics.

The balance between HR and NHEJ is essential for genome stability and tumor suppression because dysregulation of these pathways contributes to genomic instability and cancer susceptibility. Deficiencies or dysregulation of either NHEJ or HR can promote an alternative repair pathway,

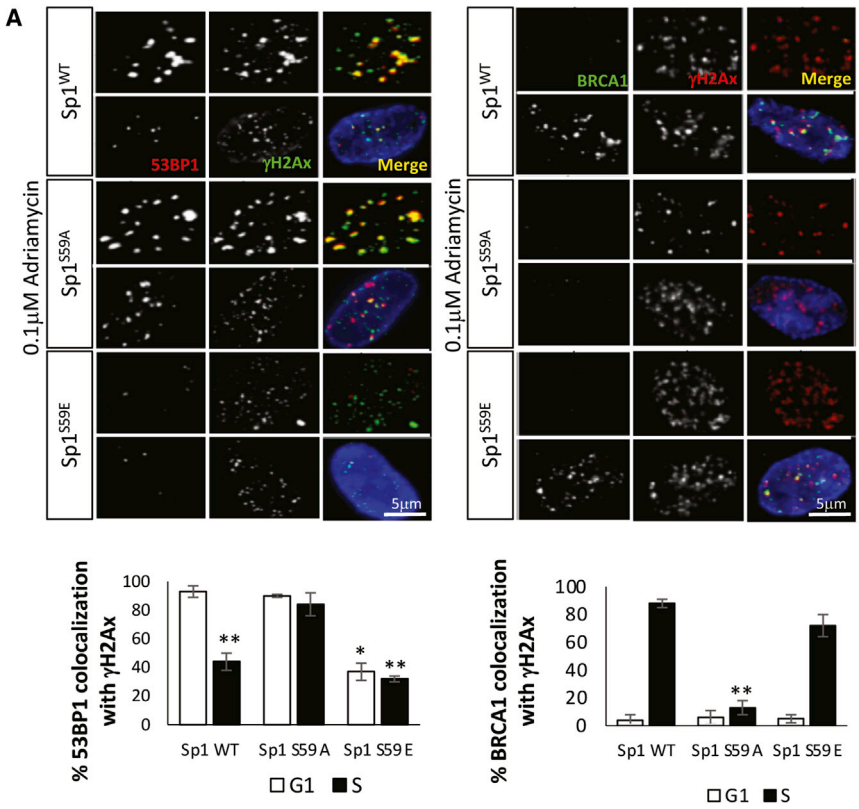

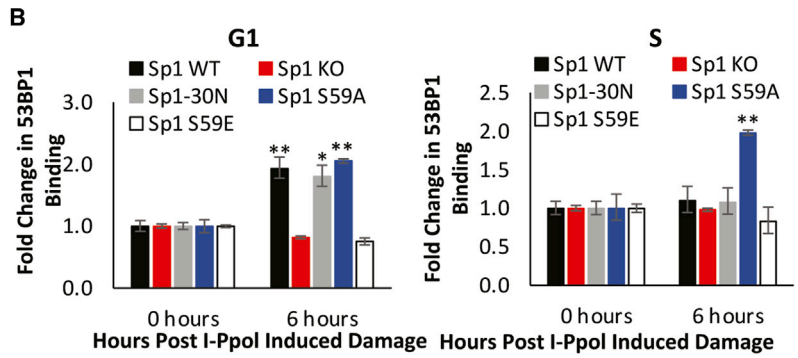

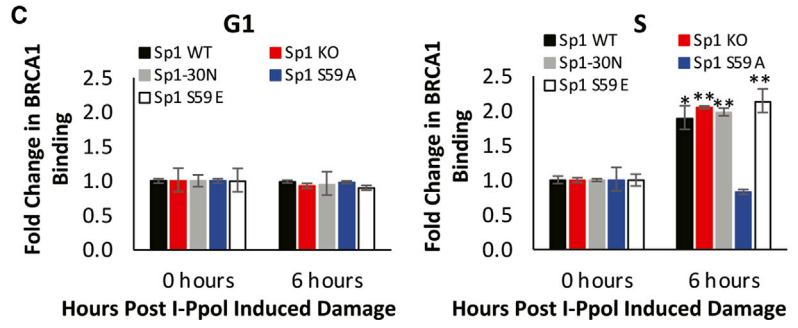

Figure 5. Sp1 acts as a cell-cycle sensor to ensure proper repair factor recruitment

(A–C) Sp1 was knocked out in U2OS cells using sgRNA targeting Sp1 and FLAG-tagged FL $Sp1^{WT}$, $Sp1^{S59A}$, $Sp1^{S59E}$ (A–C), EV, or $Sp1^{30N}$ (B and C) were expressed by lentiviral transduction.

(A) Cells were pretreated with 10 μM BrdU for 3 h. Damage was induced by treatment with 0.1 μM Adriamycin for 1 h when cells were fixed and processed for immunofluorescence using antibodies against 53BP1, BRCA1, γH2Ax, and BrdU.

(B) Sp1 was knocked out in U2OS cells using sgRNA targeting Sp1 and FLAG-tagged FL $Sp1^{WT}$, $Sp1^{S59A}$, and $Sp1^{S59E}$. These cells were transfected with GFP-53BP1 and then transduced with I-PpoI. Cells were synchronized in the G1 or S phase and treated with 4-OHT to induce DSBs. DNA was isolated from cell lysates 6 h after induction of I-PpoI, and ChIP was performed using a GFP antibody, followed by qPCR using primers adjacent to the break site.

(C) U2OS cells expressing I-PpoI described above were synchronized in the G1 or S phase and treated with 4-OHT to induce DSBs. DNA was isolated from cell lysates 6 h after induction of I-PpoI, and ChIP was performed with a BRCA1 antibody, followed by qPCR using primers adjacent to the break site.

Data represent means ± SEM from three independent experiments assessed in triplicate. For (A)–(C), statistical analysis was performed as in Figure 1.

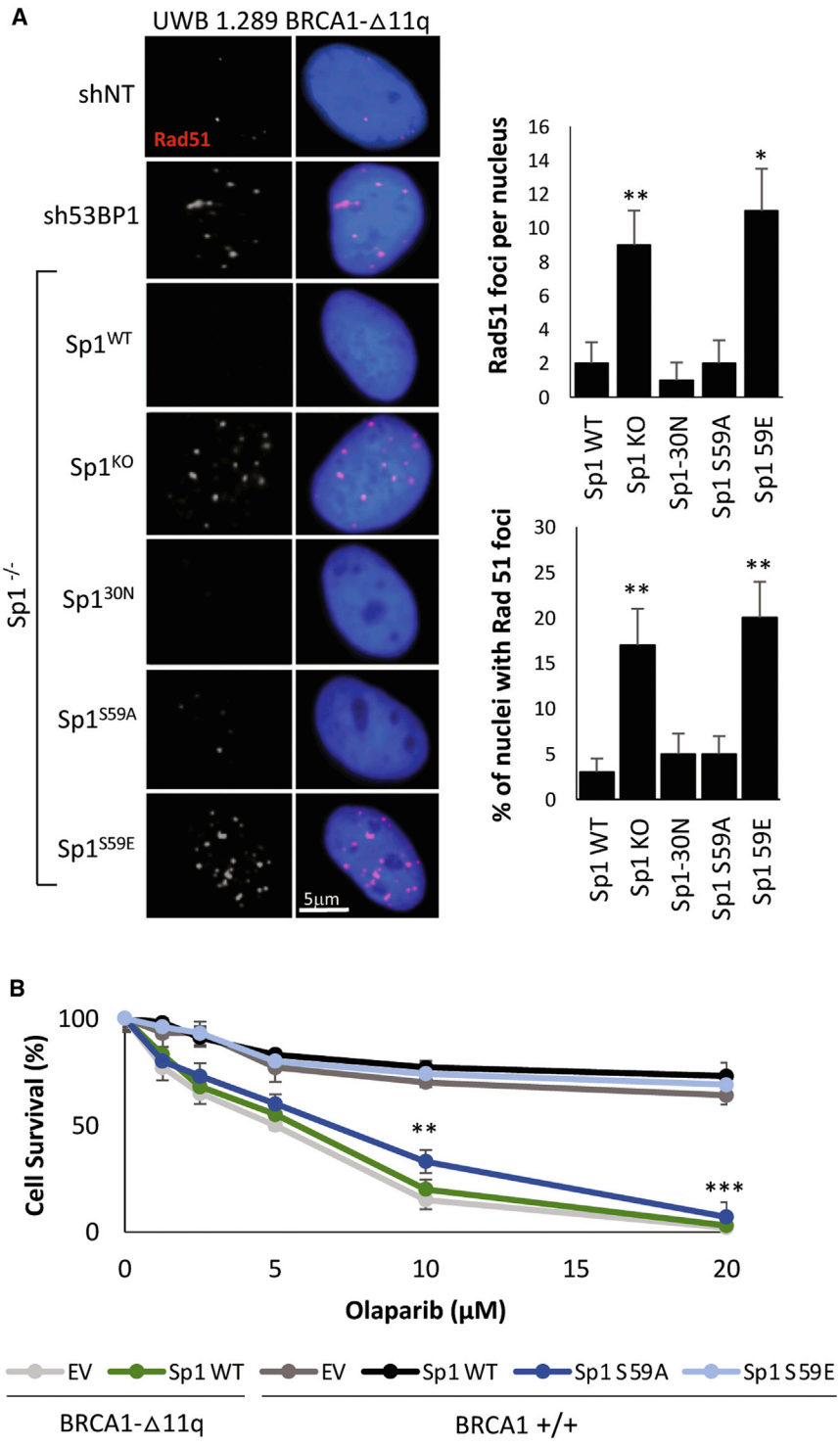

Figure 6. Sp1 acts as a cell-cycle sensor to ensure proper repair pathway choice

(A) Sp1 was knocked out in UWB 1.289 BRCA1-Δ11q cells and $Sp1^{WT}$, EV, $Sp1^{30N}$, $Sp1^{S59A}$, or $Sp1^{S59E}$ were expressed by viral transduction. Cells were treated with 0.1 μM Adriamycin for 1 h, fixed, and processed for immunofluorescence using antibody against Rad51 and stained with DAPI.

(B) Sp1 was knocked out in UWB 1.289 BRCA1-Δ11q or $BRCA1^{+/+}$ cells and $Sp1^{WT}$, $Sp1^{S59A}$, or $Sp1^{S59E}$ were expressed by lentiviral transduction (shown in Figure S6F). Cells were seeded in agar and treated with the indicated doses of olaparib. Cells were incubated for 14 days, followed by staining and quantification. Data represent means ± SEM from three independent experiments assessed in triplicate. Statistical analysis was performed as in Figure 1.

microhomology-mediated end joining (MMEJ), an error-prone pathway for DSB repair, which creates deletions flanking the break sites and contributes to chromosome translocations and rearrangements (Seol et al., 2018). Inappropriate use of NHEJ also drives genomic instability. Defects within the Fanconi anemia (FA) repair pathway for repair of DNA crosslinks results in inappropriate use of NHEJ at damaged or stalled replication forks. FA-deficient cells display radial chromosomes generated because of translocations between non-homologous chromosomes resulting from NHEJ, which can be prevented by knocking down repair proteins necessary for NHEJ (Adamo et al., 2010; Pace et al., 2010).

Here, we demonstrate that Sp1 mediates proper repair of DSBs by NHEJ. We show Sp1 recruitment to break sites in the G1 phase, when NHEJ is the predominant repair pathway. Cell-cycle-dependent phosphorylation of Sp1 in the early S phase when HR is the predominant repair pathway, promotes eviction of Sp1 and 53BP1, thereby allowing BRCA1 binding and HR. Our data support a model in which Sp1 is recruited to the break site and phosphorylated by ATM in response to damage in a G1 cell.

Sp1 is phosphorylated on S59 by cyclin A/cdk2, the activity of which peaks at the beginning of the S phase (Fojas de Borja et al., 2001). In the absence of S59 phosphorylation ($Sp1^{S59A}$), Sp1 is retained at the break site in both the G1 and the S phase indicating that S59 phosphorylation evicts Sp1 and thereby 53BP1 from DSBs. Failure to evict Sp1 and 53BP1 in the S phase, blocks BRCA1 binding, resulting in HR defects and increased sensitivity to PARP inhibition (Figures 4B and 6B). In contrast, when the cyclin A/cdk2 phosphomimetic Sp1 ($Sp1^{S59E}$) mutant is expressed, Sp1 and 53BP1 are precluded from DSBs in both the G1 and the S phase cells (Figures 5A

and 5B). When the Sp1 phosphomimetic ($Sp1^{S59E}$) is precluded from the break site, BRCA1 is recruited in the S phase cells.

The lack of BRCA1 binding in Sp1-cyclin A/cdk2 phospho-null mutants may be attributed to how BRCA1 recognizes and is recruited to DSBs. BRCA1 recognizes DSBs by interacting with the ubiquitin binding protein, Rap80. Rap80 localizes to DSBs through its tandem ubiquitin interactions motifs (UIMs), independent of BRCA1. These UIM domains are essential for Rap80 localization and binding to BRCA1 (through its BRCT domain), suggesting that ubiquitin is the targeting signal for BRCA1-Rap80 complexes (Greenberg, 2008). Future studies will address whether Sp1 binds to and blocks ubiquitination of Rap80, thereby precluding BRCA1 from being recruited to DSBs.

Phosphorylation of the end-resection repair factor CtIP is also regulated via the cell cycle. Phosphorylation of CtIP by cyclin A/cdk2 is necessary for stabilizing and activating its role in recruiting other factors necessary for end-resection, enabling HR-mediated repair in S phase. Upon phosphorylation of CtIP by cyclin A/cdk2, the MRN-CtIP-BRCA1 end-resection complex assembles, and HR is initiated. Cdk2 interacts directly with Mre11 of the MRN complex, regulating CtIP phosphorylation and BRCA1 interaction in dividing cells (Buis et al., 2012). We have preliminary data to support that Sp1 interacts with and is stabilized via its interaction with Nbs1, another member of the MRN complex. At DSBs, that interaction and stabilization should only occur in G1 because Sp1 is removed from DSBs in the S phase cells. Whether cdk2-mediated phosphorylation of CtIP to promote its interaction with the MRN complex for end resection and the phosphorylation of Sp1 at S59 for the removal of Sp1 from DSBs are related to Sp1's interaction and stabilization by Nbs1 and its interaction with Mre11 and CtIP in the S phase requires further investigation.

Moreover, Sp1-S59 is dephosphorylated by the phosphatase PP2A (Vicart et al., 2006). Regulating almost all major pathways and cell-cycle checkpoints, PP2A is known to dephosphorylate more than 300 substrates involved in the cell cycle and is a master regulator of the cell cycle by competing for the same docking sites as CDKs (Feng et al., 2009; Garriga et al., 2004; Wlodarchak and Xing, 2016). This reversible phosphorylation of proteins, catalyzed by protein kinases and phosphatases, is also a major mechanism for regulating DSB repair (Wang et al., 2009). PP2A directly dephosphorylates Ku and DNA-PKcs (a catalytic subunit), enhancing formation of a functional Ku/DNA-PKcs complex and NHEJ (Chowdhury et al., 2005; Douglas et al., 2001; Wang et al., 2009). Therefore, PP2A may also have a role in dephosphorylation of Sp1 at serine 59 in G1 to ensure proper repair choice pathway.

53BP1 is necessary for the synthetic lethality between mutant BRCA1 and PARP inhibition because BRCA1-Δ11q cells that also are defective in 53BP1 recruitment display PARP inhibitor resistance (Nacson et al., 2018). Therefore, we hypothesized that BRCA-Δ11q cells expressing the $Sp1^{S59E}$, which fail to recruit 53BP1 (Figure 5), would also be resistant to PARP inhibition. However, Sp1 knockout resulted in the death of UWB 1.289 BRCA-Δ11q, indicating that Sp1 knockout is a synthetic lethal with BRCA1 mutation, similar to the synthetic lethality with PARP inhibition. This suggests that Sp1 may be involved in other repair processes, such as repair of single-strand breaks or transcription-coupled repair. Deficiencies in either of these repair pathways combined with BRCA1 mutagenesis also lead to increased cell death (Barnes and Lindahl, 2004). Future studies will investigate whether Sp1 in involved in either of these repair processes and determine how it causes synthetic lethality with BRCA1 mutation.

Although the exact mechanism by which a cell senses a DSB is not entirely clear, previous data suggest that alterations in chromatin structure result in the activation of ATM through its autophosphorylation and monomerization (Bensimon et al., 2010). Activation of ATM elicits widespread cell responses through phosphorylation of downstream effector proteins for either activating or recruiting those factors to DSBs (Bensimon et al., 2010; Lee and Paull, 2005). Previously, we showed that Sp1 is phosphorylated by ATM at Ser101, although that phosphorylation was not necessary for the recruitment of Sp1 to DSBs (Beishline et al., 2012). Future experiments will determine whether phosphorylation by ATM initiates other downstream interactions or post-translational modifications that mediate Sp1's activity within the DSB repair process. We have evidence to support that, similar to its role as a transcription factor, $Sp1^{pS101}$ interacts with, and is necessary for, recruiting the histone acetylase p300, a chromatin modifier that acetylates both histones H3 and H4 necessary for DNA repair factor binding. This could suggest that Sp1 modulates NHEJ repair factor recruitment through its interaction with chromatin modifiers and modulating the chromatin landscape.

Here, we demonstrate a previously unidentified mechanism that integrates the cell cycle and DSB repair pathway choice. We have shown that phosphorylation of Sp1 in the S phase evicts Sp1 and 53BP1 from the break site and inhibits NHEJ repair. Mutations of the cyclin A/cdk2 phosphorylation site on Sp1 result in aberrant repair factor binding to DSB sites. We hypothesize that Sp1 is evicted from DSB sites in a cell-cycle-specific manner to prevent inappropriate 53BP1 binding and NHEJ in S phase, thereby allowing BRCA1 recruitment and HR. This switch couples the cell cycle to DNA repair pathway choice to ensure that the proper repair pathway is used in each cell cycle phase.

In summary, we have demonstrated that Sp1 is necessary for DSB repair via NHEJ. Sp1 mediates 53BP1 binding and retention at the break site. In addition, the phosphorylation of Sp1 by the cyclin A/cdk2 complex provides a mechanism by which the cell cycle regulates DNA repair pathway choice. Future experiments will determine how the cell cycle affects Sp1's role in modifying the chromatin landscape for NHEJ repair-factor binding.

STAR★METHODS

Detailed methods are provided in the online version of this paper and include the following:

- KEY RESOURCES TABLE
- RESOURCE AVAILABILITY
  - Lead contact
  - Materials availability

SUPPLEMENTAL INFORMATION

Supplemental information can be found online at https://doi.org/10.1016/j.celrep.2021.108840.

ACKNOWLEDGMENTS

The authors thank Mauricio Reginato, Alexander Mazin, Eishi Noguchi, Jiri Lukas, Jeremy Stark, and Jeong-Heon Lee for their generous donation of DNA constructs, cells, and antibodies, which were essential for this study. In addition, we thank Alex Mazin, Christine Eischen, and Roger Greenberg for helpful suggestions and Kelly Donovan for intellectual input, manuscript editing, and construction of the pLZS-Sp1 construct. M.L.S. is funded by the Drexel University College of Medicine Aging Initiative Graduate Student Fellowship.

AUTHOR CONTRIBUTIONS

Conceptualization, M.L.S., K.B., and J.A.-C.; methodology, M.L.S. and J.A.-C.; investigation, M.L.S. and S.F.; writing – original draft and review & editing, M.L.S. and J.A.-C.; supervision, J.A.-C.

DECLARATION OF INTERESTS

The authors declare no competing interest.

Received: March 12, 2020
Revised: September 13, 2020
Accepted: February 17, 2021
Published: March 16, 2021

REFERENCES

Adachi, N., Suzuki, H., Iiizumi, S., and Koyama, H. (2003). Hypersensitivity of nonhomologous DNA end-joining mutants to VP-16 and ICRF-193: implications for the repair of topoisomerase II-mediated DNA damage. J. Biol. Chem. *278*, 35897–35902.

Adachi, N., Iiizumi, S., So, S., and Koyama, H. (2004). Genetic evidence for involvement of two distinct nonhomologous end-joining pathways in repair of topoisomerase II-mediated DNA damage. Biochem. Biophys. Res. Commun. *318*, 856–861.

Adamo, A., Collis, S.J., Adelman, C.A., Silva, N., Horejsi, Z., Ward, J.D., Martinez-Perez, E., Boulton, S.J., and La Volpe, A. (2010). Preventing nonhomologous end joining suppresses DNA repair defects of Fanconi anemia. Mol. Cell *39*, 25–35.

Agami, R., and Bernards, R. (2000). Distinct initiation and maintenance mechanisms cooperate to induce G1 cell cycle arrest in response to DNA damage. Cell *102*, 55–66.

Baer, R., and Ludwig, T. (2002). The BRCA1/BARD1 heterodimer, a tumor suppressor complex with ubiquitin E3 ligase activity. Curr. Opin. Genet. Dev. *12*, 86–91.

Banchio, C., Schang, L.M., and Vance, D.E. (2004). Phosphorylation of Sp1 by cyclin-dependent kinase 2 modulates the role of Sp1 in CTP:phosphocholine cytidylyltransferase alpha regulation during the S phase of the cell cycle. J. Biol. Chem. *279*, 40220–40226.

Barnes, D.E., and Lindahl, T. (2004). Repair and genetic consequences of endogenous DNA base damage in mammalian cells. Annu. Rev. Genet. *38*, 445–476.

Beishline, K., and Azizkhan-Clifford, J. (2014). Interplay between the cell cycle and double-strand break response in mammalian cells. Methods Mol. Biol. *1170*, 41–59.

Beishline, K., Kelly, C.M., Olofsson, B.A., Koduri, S., Emrich, J., Greenberg, R.A., and Azizkhan-Clifford, J. (2012). Sp1 facilitates DNA double-strand break repair through a nontranscriptional mechanism. Mol. Cell. Biol. *32*, 3790–3799.

Bennardo, N., Cheng, A., Huang, N., and Stark, J.M. (2008). Alternative-NHEJ is a mechanistically distinct pathway of mammalian chromosome break repair. PLoS Genet. *4*, e1000110.

Bennett, G., Papamichos-Chronakis, M., and Peterson, C.L. (2013). DNA repair choice defines a common pathway for recruitment of chromatin regulators. Nat. Commun. *4*, 2084.

Bensimon, A., Schmidt, A., Ziv, Y., Elkon, R., Wang, S.Y., Chen, D.J., Aebersold, R., and Shiloh, Y. (2010). ATM-dependent and -independent dynamics of the nuclear phosphoproteome after DNA damage. Sci. Signal. *3*, rs3.

Berkovich, E., Monnat, R.J., Jr., and Kastan, M.B. (2007). Roles of ATM and NBS1 in chromatin structure modulation and DNA double-strand break repair. Nat. Cell Biol. *9*, 683–690.

Bhargava, R., Sandhu, M., Muk, S., Lee, G., Vaidehi, N., and Stark, J.M. (2018). C-NHEJ without indels is robust and requires synergistic function of distinct XLF domains. Nat. Commun. *9*, 2484.

Black, A.R., Black, J.D., and Azizkhan-Clifford, J. (2001). Sp1 and krüppel-like factor family of transcription factors in cell growth regulation and cancer. J. Cell. Physiol. *188*, 143–160.

Bouwman, P., and Philipsen, S. (2002). Regulation of the activity of Sp1-related transcription factors. Mol. Cell. Endocrinol. *195*, 27–38.

Bouwman, P., Aly, A., Escandell, J.M., Pieterse, M., Bartkova, J., van der Gulden, H., Hiddingh, S., Thanasoula, M., Kulkarni, A., Yang, Q., et al. (2010). 53BP1 loss rescues BRCA1 deficiency and is associated with triple-negative and BRCA-mutated breast cancers. Nat. Struct. Mol. Biol. *17*, 688–695.

Branzei, D., and Foiani, M. (2008). Regulation of DNA repair throughout the cell cycle. Nat. Rev. Mol. Cell Biol. *9*, 297–308.

Britton, S., Coates, J., and Jackson, S.P. (2013). A new method for high-resolution imaging of Ku foci to decipher mechanisms of DNA double-strand break repair. J. Cell Biol. *202*, 579–595.

Buis, J., Stoneham, T., Spehalski, E., and Ferguson, D.O. (2012). Mre11 regulates CtIP-dependent double-strand break repair by interaction with CDK2. Nat. Struct. Mol. Biol. *19*, 246–252.

Bunting, S.F., Callén, E., Wong, N., Chen, H.T., Polato, F., Gunn, A., Bothmer, A., Feldhahn, N., Fernandez-Capetillo, O., Cao, L., et al. (2010). 53BP1 inhibits homologous recombination in Brca1-deficient cells by blocking resection of DNA breaks. Cell *141*, 243–254.

Chapman, J.R., Barral, P., Vannier, J.B., Borel, V., Steger, M., Tomas-Loba, A., Sartori, A.A., Adams, I.R., Batista, F.D., and Boulton, S.J. (2013). RIF1 is essential for 53BP1-dependent nonhomologous end joining and suppression of DNA double-strand break resection. Mol. Cell *49*, 858–871.

Chowdhury, D., Keogh, M.C., Ishii, H., Peterson, C.L., Buratowski, S., and Lieberman, J. (2005). gamma-H2AX dephosphorylation by protein phosphatase 2A facilitates DNA double-strand break repair. Mol. Cell *20*, 801–809.

Costa, A.R., Machado, N., Rego, A., Sousa, M.J., Côrte-Real, M., and Chaves, S.R. (2019). Proteasome inhibition prevents cell death induced by the chemotherapeutic agent cisplatin downstream of DNA damage. DNA Repair (Amst.) *73*, 28–33.

Deniaud, E., Baguet, J., Chalard, R., Blanquier, B., Brinza, L., Meunier, J., Michallet, M.C., Laugraud, A., Ah-Soon, C., Wierinckx, A., et al. (2009). Overexpression of transcription factor Sp1 leads to gene expression perturbations and cell cycle inhibition. PLoS ONE *4*, e7035.

Douglas, P., Moorhead, G.B., Ye, R., and Lees-Miller, S.P. (2001). Protein phosphatases regulate DNA-dependent protein kinase activity. J. Biol. Chem. *276*, 18992–18998.

Feng, J., Wakeman, T., Yong, S., Wu, X., Kornbluth, S., and Wang, X.F. (2009). Protein phosphatase 2A-dependent dephosphorylation of replication protein A is required for the repair of DNA breaks induced by replication stress. Mol. Cell. Biol. *29*, 5696–5709.

Feng, L., Li, N., Li, Y., Wang, J., Gao, M., Wang, W., and Chen, J. (2015). Cell cycle-dependent inhibition of 53BP1 signaling by BRCA1. Cell Discov. *1*, 15019.

Fletcher, S.C., Grou, C.P., Legrand, A.J., Chen, X., Soderstrom, K., Poletto, M., and Dianov, G.L. (2018). Sp1 phosphorylation by ATM downregulates BER and promotes cell elimination in response to persistent DNA damage. Nucleic Acids Res. *46*, 1834–1846.

Fojas de Borja, P., Collins, N.K., Du, P., Azizkhan-Clifford, J., and Mudryj, M. (2001). Cyclin A-CDK phosphorylates Sp1 and enhances Sp1-mediated transcription. EMBO J. *20*, 5737–5747.

Garriga, J., Jayaraman, A.L., Limón, A., Jayadeva, G., Sotillo, E., Truongcao, M., Patsialou, A., Wadzinski, B.E., and Graña, X. (2004). A dynamic equilibrium between CDKs and PP2A modulates phosphorylation of pRB, p107 and p130. Cell Cycle *3*, 1320–1330.

Greenberg, R.A. (2008). Recognition of DNA double strand breaks by the BRCA1 tumor suppressor network. Chromosoma *117*, 305–317.

Gulbranson, D.R., Davis, E.M., Demmitt, B.A., Ouyang, Y., Ye, Y., Yu, H., and Shen, J. (2017). RABIF/MSS4 is a Rab-stabilizing holdase chaperone required for GLUT4 exocytosis. Proc. Natl. Acad. Sci. USA *114*, E8224–E8233.

Her, J., and Bunting, S.F. (2018). How cells ensure correct repair of DNA double-strand breaks. J. Biol. Chem. *293*, 10502–10511.

Kalderon, D., Roberts, B.L., Richardson, W.D., and Smith, A.E. (1984). A short amino acid sequence able to specify nuclear location. Cell *39*, 499–509.

Kang, D.S., Hong, K.M., Park, J., and Bae, C.D. (2012). Cyclin A regulates a cell-cycle-dependent expression of CKAP2 through phosphorylation of Sp1. Biochem. Biophys. Res. Commun. *420*, 822–827.

Karanam, K., Kafri, R., Loewer, A., and Lahav, G. (2012). Quantitative live cell imaging reveals a gradual shift between DNA repair mechanisms and a maximal use of HR in mid S phase. Mol. Cell *47*, 320–329.

Kim, H.S., and Lim, I.K. (2009). Phosphorylated extracellular signal-regulated protein kinases 1 and 2 phosphorylate Sp1 on serine 59 and regulate cellular senescence via transcription of p21Sdi1/Cip1/Waf1. J. Biol. Chem. *284*, 15475–15486.

Kim, S.T., Lim, D.S., Canman, C.E., and Kastan, M.B. (1999). Substrate specificities and identification of putative substrates of ATM kinase family members. J. Biol. Chem. *274*, 37538–37543.

Krais, J.J., Wang, Y., Bernhardy, A.J., Clausen, E., Miller, J.A., Cai, K.Q., Scott, C.L., and Johnson, N. (2020). RNF168-mediated ubiquitin signaling inhibits the viability of *BRCA1*-null cancers. Cancer Res. *80*, 2848–2860.

Lee, J.H., and Paull, T.T. (2005). ATM activation by DNA double-strand breaks through the Mre11-Rad50-Nbs1 complex. Science *308*, 551–554.

Lin, S.Y., Black, A.R., Kostic, D., Pajovic, S., Hoover, C.N., and Azizkhan, J.C. (1996). Cell cycle-regulated association of E2F1 and Sp1 is related to their functional interaction. Mol. Cell. Biol. *16*, 1668–1675.

Liu, S., Fan, Z., Geng, Z., Zhang, H., Ye, Q., Jiao, S., and Xu, X. (2013). PIAS3 promotes homology-directed repair and distal non-homologous end joining. Oncol. Lett. *6*, 1045–1048.

Maede, Y., Shimizu, H., Fukushima, T., Kogame, T., Nakamura, T., Miki, T., Takeda, S., Pommier, Y., and Murai, J. (2014). Differential and common DNA repair pathways for topoisomerase I- and II-targeted drugs in a genetic DT40 repair cell screen panel. Mol. Cancer Ther. *13*, 214–220.

Mujoo, K., Pandita, R.K., Tiwari, A., Charaka, V., Chakraborty, S., Singh, D.K., Hambarde, S., Hittelman, W.N., Horikoshi, N., Hunt, C.R., et al. (2017). Differentiation of human induced pluripotent or embryonic stem cells decreases the DNA damage repair by homologous recombination. Stem Cell Reports *9*, 1660–1674.

Nacson, J., Krais, J.J., Bernhardy, A.J., Clausen, E., Feng, W., Wang, Y., Nicolas, E., Cai, K.Q., Tricarico, R., Hua, X., et al. (2018). BRCA1 mutation-specific responses to 53BP1 loss-induced homologous recombination and PARP inhibitor resistance. Cell Rep. *25*, 1384.

Nelson, J.D., Denisenko, O., and Bomsztyk, K. (2006). Protocol for the fast chromatin immunoprecipitation (ChIP) method. Nat. Protoc. *1*, 179–185.

Olofsson, B.A., Kelly, C.M., Kim, J., Hornsby, S.M., and Azizkhan-Clifford, J. (2007). Phosphorylation of Sp1 in response to DNA damage by ataxia telangiectasia-mutated kinase. Mol. Cancer Res. *5*, 1319–1330.

Pace, P., Mosedale, G., Hodskinson, M.R., Rosado, I.V., Sivasubramaniam, M., and Patel, K.J. (2010). Ku70 corrupts DNA repair in the absence of the Fanconi anemia pathway. Science *329*, 219–223.

Qi, W., Chen, H., Xiao, T., Wang, R., Li, T., Han, L., and Zeng, X. (2016). Acetyltransferase p300 collaborates with chromodomain helicase DNA-binding protein 4 (CHD4) to facilitate DNA double-strand break repair. Mutagenesis *31*, 193–203.

Sanjana, N.E., Shalem, O., and Zhang, F. (2014). Improved vectors and genome-wide libraries for CRISPR screening. Nat. Methods *11*, 783–784.

Schultz, L.B., Chehab, N.H., Malikzay, A., and Halazonetis, T.D. (2000). p53 binding protein 1 (53BP1) is an early participant in the cellular response to DNA double-strand breaks. J. Cell Biol. *151*, 1381–1390.

Seol, J.H., Shim, E.Y., and Lee, S.E. (2018). Microhomology-mediated end joining: good, bad and ugly. Mutat. Res. *809*, 81–87.

Shields, J.M., and Yang, V.W. (1997). Two potent nuclear localization signals in the gut-enriched Krüppel-like factor define a subfamily of closely related Krüppel proteins. J. Biol. Chem. *272*, 18504–18507.

Smogorzewska, A., and de Lange, T. (2002). Different telomere damage signaling pathways in human and mouse cells. EMBO J. *21*, 4338–4348.

Spengler, M.L., Guo, L.W., and Brattain, M.G. (2008). Phosphorylation mediates Sp1 coupled activities of proteolytic processing, desumoylation and degradation. Cell Cycle *7*, 623–630.

Torabi, B., Flashner, S., Beishline, K., Sowash, A., Donovan, K., Bassett, G., and Azizkhan-Clifford, J. (2018). Caspase cleavage of transcription factor Sp1 enhances apoptosis. Apoptosis *23*, 65–78.

van den Heuvel, S., and Harlow, E. (1993). Distinct roles for cyclin-dependent kinases in cell cycle control. Science *262*, 2050–2054.

Vicart, A., Lefebvre, T., Imbert, J., Fernandez, A., and Kahn-Perlès, B. (2006). Increased chromatin association of Sp1 in interphase cells by PP2A-mediated dephosphorylations. J. Mol. Biol. *364*, 897–908.

Wang, Q., Gao, F., Wang, T., Flagg, T., and Deng, X. (2009). A nonhomologous end-joining pathway is required for protein phosphatase 2A promotion of DNA double-strand break repair. Neoplasia *11*, 1012–1021.

Wang, Y.T., Yang, W.B., Chang, W.C., and Hung, J.J. (2011). Interplay of post-translational modifications in Sp1 mediates Sp1 stability during cell cycle progression. J. Mol. Biol. *414*, 1–14.

Wlodarchak, N., and Xing, Y. (2016). PP2A as a master regulator of the cell cycle. Crit. Rev. Biochem. Mol. Biol. *51*, 162–184.

Wu-Baer, F., Lagrazon, K., Yuan, W., and Baer, R. (2003). The BRCA1/BARD1 heterodimer assembles polyubiquitin chains through an unconventional linkage involving lysine residue K6 of ubiquitin. J. Biol. Chem. *278*, 34743–34746.

Xia, Z., Morales, J.C., Dunphy, W.G., and Carpenter, P.B. (2001). Negative cell cycle regulation and DNA damage-inducible phosphorylation of the BRCT protein 53BP1. J. Biol. Chem. *276*, 2708–2718.

Zong, D., Adam, S., Wang, Y., Sasanuma, H., Callén, E., Murga, M., Day, A., Kruhlak, M.J., Wong, N., Munro, M., et al. (2019). BRCA1 Haploinsufficiency Is Masked by RNF168-Mediated Chromatin Ubiquitylation. Mol. Cell *73*, 1267–1281.e7.

STAR★METHODS

KEY RESOURCES TABLE

REAGENT or RESOURCE	SOURCE	IDENTIFIER
Antibodies		
53BP1 (Western Blot and Immunofluorescence)	Millipore	Cat# MAB3802; RRID:AB_2206767
BRCA1 (Immunofluorescence and ChIP)	Novus Biologicals	Cat# NB100-404; RRID:AB_10003091
BRCA1 (Western Blot and Immunofluorescence)	Santa Cruz	sc-642; RRID:AB_630944
Brdu (Immunofluorescence)	Abcam	ab6326; RRID:AB_305426
Chk2 (Western Blot)	Cell Signaling Tech	Cat# 3440; RRID:AB_2229490
Cyclin A (Western Blot)	Millipore Sigma	Cat# 06-138; RRID:AB_310058
Cyclin E (Western Blot)	Santa Cruz	Cat# sc-377101
DNA-PK (Western Blot and Immunofluorescence)	EMD Millipore	NA57; RRID:AB_2172815
Flag-M2 (CoIP and ChIP)	Sigma-Aldrich	Cat# A2220; RRID:AB_10063035
Flag-M2 (Western Blot)	Millipore-Sigma	Cat# F1804; RRID:AB_262044
GFP (ChIP)	Abcam	Cat# ab290; RRID:AB_303395
GFP (Western Blot)	Santa Cruz	Cat# sc-9996; RRID:AB_627695
HA (Western Blot)	Cell Signaling Tech	Cat# 2367; RRID:AB_10691311
IgG control (ChIP)	Abcam	Cat# ab171870; RRID:AB_2687657
Ku70 (Western Blot)	Santa Cruz	Cat# sc-5309; RRID:AB_628453
Nbs1 (ChIP)	Invitrogen	Cat# MA1-23265; RRID:AB_560310
Nbs1 (Western Blot)	Santa Cruz	Cat# sc-374168; RRID:AB_10989764
Phosho-Chk2 (Western Blot)	Cell Signaling Tech	Cat# 2197; RRID:AB_2080501
Rad51 (Immunofluorescence)	Abcam	ab1837; RRID:AB_302635
Rad54 (Western Blot)	Santa Cruz	sc-374598; RRID:AB_10989787
α-tubulin (Western Blot)	Cell Signaling Tech	Cat# 2144; RRID:AB_2210548
γH2Ax (Immunofluorescence and ChIP)	Millipore-Sigma	Cat# 05-636; RRID:AB_309864
γH2Ax (Immunofluorescence)	Abcam	Cat# ab11174; RRID:AB_297813
γH2Ax (Western Blot)	Biolegend	Cat# 613402; RRID:AB_315795
Chemicals, peptides, and recombinant proteins		
4-OHT	Sigma	H6278
RO-3306	Selleckchem	S7747
Experimental models: cell lines		
293 GPG	Richard Mulligan	N/A
293T	ATCC	Cat# CRL-3216; RRID:CVCL_0063
hTert RPE-1	ATCC	Cat# CRL-4000; RRID:CVCL_4388
U-2 OS	ATCC	Cat# HTB-96; RRID:CVCL_0042
UWB 1.289	ATCC	Cat# CRL-2945; RRID:CVCL_B079
UWB 1.289+BRCA1	ATCC	Cat# CRL-2946; RRID:CVCL_B078
Oligonucleotides		
sgSp1 F: 5′ CACCGCATGGATGAAATGACAGCTG 3′	Eurofins	N/A
sgSp1 R: 5′ AAACCAGCTGTCATTTCATCCATGC 3′	Eurofins	N/A
Recombinant DNA		
7a sgRNA for EJ7-GFP reporter	Addgene	113620
7b sgRNA for EJ7-GFP reporter	Addgene	113624
Cdk2-DN-HA	Addgene	1885
Cdk2-HA	Addgene	1884
lentiCRISPR v2	Addgene	52961

(*Continued on next page*)

Continued

REAGENT or RESOURCE	SOURCE	IDENTIFIER
pBABE-HA-ER-I-PpoI	Addgene	32565
pCMV-A-puro-GFP-C1-53BP1	Juri Lukas	N/A
pLenti CMV GFP Zeo	Addgene	17449
pLKO-shRNA Sp1 1805	Sigma	TRCN0000020448
pLKO-shRNA Sp1 7276	Sigma	TRCN0000020446
pLPC-NMYC TRF2ΔBΔM	Addgene	16069

RESOURCE AVAILABILITY

Lead contact

Further information and request for resources and reagents should be directed and will be fulfilled by the lead contact, Dr. Jane Aziz-khan-Clifford (jane.clifford@drexel.edu).

Materials availability

The unique reagents and strains generated in this study are available from the lead contact upon request.

Data and code availability

This study did not generate/analyze datasets/code.

EXPERIMENTAL MODELS AND SUBJECT DETAILS

Cells

Human osteosarcoma cell line U2OS (ATCC) was cultured in high glucose Dulbecco's modified Eagle's medium (DMEM 10-013; Corning) containing 10% FBS (Gemini), 0.1mg/mL penicillin, and 60 g/mL streptomycin (Pen-Strep). Cells were incubated at 37°C in a humidified atmosphere of 5% CO_2. Retinal epithelial immortalized with hTert (hTert RPE-1) cell line was cultured in DMEM:F12 medium (Corning; 10-090) containing 10% FBS (Gemini), 0.1mg/mL hygromycin B, 0.1mg/mL penicillin, and 60 g/mL streptomycin (Pen-Strep) at 37°C in a humidified atmosphere of 5% CO_2. Human ovarian carcinoma cells, UWB 1.289 (kind gift from Alexander Mazin, Drexel University College of Medicine, Pennsylvania, USA) were cultured in 50% RPMI-1640 media (Corning 10-0400), 50% MEGM media (Lonza CC-3150), and 3% FBS at 37°C in a humidified atmosphere of 5% CO_2. The viral packaging cell line 293-GPG was maintained in DMEM containing 2mM L-glutamine, 110mg/mL sodium pyruvate, 10% heat inactivated FBS (Gemini), Pen-Strep, 1 μg/mL tetracycline, 2 μg/mL puromycin, and 0.3mg/mL G418 at 37°C in a humidified atmosphere of 5% CO_2. During production of retroviruses or lentiviruses, 293-GPG and HEK293T cells were maintained in DMEM containing 2mM L-glutamine, 110mg/mL sodium pyruvate, and 10% heat inactivated FBS (Gemini). During infection of U2OS cells with I-PpoI endonuclease fusion construct and treatment with 4-hydroxytamoxifen (4-OHT), cells were maintained in phenol-free DMEM (GIBCO) with 10% charcoal stripped FBS (Gemini).

METHOD DETAILS

Plasmid constructs

The pBABE-HA-ER-I-PpoI and pLPC-NMYC TRF2ΔBΔM plasmids were purchased from Addgene (32565 and 16069) (Berkovich et al., 2007; Smogorzewska and de Lange, 2002). The pCMV-A-puro-GFP-C1-53BP1 construct was kindly provided by J. Lukas (University of Copenhagen, Denmark). The 7a and 7b sgRNA for EJ7-GFP constructs were purchased from Addgene (113620 and 113624) (Bhargava et al., 2018). The Cdk2-HA and Cdk2-DN-HA constructs were also purchased from Addgene (1884 and 1885) (van den Heuvel and Harlow, 1993) pLKO-shRNA vectors for Sp1 shRNA sequences were acquired from Sigma, and targets begin at nucleic acid 1805 (coding region, number 1) and 7276 (3′ long terminal repeat [LTR], number 2) of the Sp1 mRNA sequence. Viral packaging vectors, pCMV-VSV-G, pRSV-Rev, and pMDLg/pRRE, were generously donated by M. Reginato (Drexel University College of Medicine, Pennsylvania, USA). pLXSN-Sp1-30N (182 N-terminal peptide sequence) was constructed from pLXSN-Flag-Sp1-HA. pLZS-Sp1-30N (Torabi et al., 2018) and Sp1 point mutants were constructed from pLZS-Flag-Sp1. Sp1-30N was constructed by inserting Sal1 restriction sites adjacent to codon 183 of the Sp1 sequence using PCR and the following primers: Forward (5′ CCC ACA GTT CCA GAC CGT CGA CGG GCA ACA GCT GCA G 3′) and Reverse (5′ CTG CAG CTG TTG CCC GTC GAC GGT CTG GAA CTG TGG G 3′). An additional Sal1 site was inserted along with a nuclear localization signal (Kalderon et al., 1984) since the region reportedly required for nuclear localization of Sp1 is not in the first 182 amino acids (Shields and Yang, 1997). This was done using PCR and the following primers: Forward (5′ CAG TGG CAA TGG CTT CGT CGA CCC AAA GAA GAA GCG CAA GGT CTA CCC ATA CGA TGT

TCC AG 3′) and Reverse (5′ CTG GAA CAT CGT ATG GGT AGA CCT TGC GCT TCT TCT TTG GGT CGA CGA AGC CAT TGC CAC TG 3′). Mutated Sp1 vector was then cut with SalI and self-ligated to make Flag-Sp1Δ1-182 (Sp1-30N). Sp1 sgRNA constructs were made using lentiCRISPR v2 (Addgene 52961) (Sanjana et al., 2014). Plasmid was cut using Bsmb1 and ligated to oligomers with the following sequence for Sp1: Forward (5′ CAC CGC ATG GAT GAA ATG ACA GCT G 3′) and Reverse (5′ AAA CCA GCT GTC ATT TCA TCC ATG C 3′), XRCC6: Forward (5′ GCT AGA GCT CGA CCA GTT TA 3′) and Reverse (5′ TAA ACT GGT CGA GCT CTA GC 3′) (Sanjana et al., 2014), and non-targeting: Forward(5′ CAC CGG AGC CCG ACT AAA GAG GCC G 3′) and Reverse (5′ AAA CCG GCC TCT TTA GTC GGG CTC C 3′) (Ctrl00895) (Gulbranson et al., 2017). Flag-tag in lentiCRISPr v2 with sgRNA constructs was deleted by excising Flag-Cas9 using restriction enzymes Age1 and BamH1. Product was then used for PCR using the primers: Forward (5′ AGG ACC GGT TCT AGA GCG CTG 3′) and Reverse (5′ CGT GGA TTC TTT CTT CTT AGC 3′). Product was trimmed to have compatible ends with Age1 and BamH1 and ligated into linear backbone from the original digest. pLZS-Sp1 PAM site was mutated to avoid targeting exogenous Sp1 by Cas9.

Viral production

293GPG cells were transfected with 10 μg of plasmid using GenDrill transfection reagent (BamaGen) following the manufacturer's instructions. Virus was collected on days 4 to 7 after transfection and stored frozen at −80°C. HEK293T cells were transfected with 10 μg of plasmid using GenDrill transfection reagent (BamaGen) following the manufacturer's instructions, along with viral packaging vectors pCMV-VSV-G, pRSV-Rev, and pMDLg/pRRE (kindly provided by Mauricio Reginato, Drexel University College of Medicine, PA, USA). Virus was collected 48 hours post-transfection and stored at −80°C.

Transfections

U2OS cells were transfected with 5 μg of pCMV6-A-puro-GFP-C1-53BP1 (kind gift from Jiri Lukas, University of Copenhagen, Denmark), 7a and 7b sgRNA for EJ7-GFP (Addgene 113620 and 113624) (Bhargava et al., 2018), or Cdk2-HA and Cdk2-DN-HA (Addgene 1884 and 1885) (van den Heuvel and Harlow, 1993) using Lipofectamine 3000 (ThermoFisher) following the manufacturer's instructions.

Antibodies and western blot analysis

Protein lysates were collected in 2X SDS buffer (12.5mM Tris [pH 6.8], 20% glycerol, 4% [wt/vol] SDS), and protein concentration determined by BCA assay. Proteins were separated by traditional SDS-PAGE, transferred to polyvinylidene difluoride (PVDF) membrane, blocked in 5% BSA in tris-buffered saline with Tween-20 (TBST), and probed with primary antibodies overnight at 4°C with the following antibodies: Sp1 (pAb581) (Lin et al., 1996), γH2Ax (Biolegend 613402), α-tubulin (Cell Signaling Technology 2144), Flag-M2 (Sigma-Aldrich F1804), phospho-Chk2 T68 (Cell Signaling Technology 2197), Chk2 (Cell Signaling Technology 3440), BRCA1 (Santa Cruz A2805), 53BP1 (Millipore MAB3802), Nbs1 (Santa Cruz sc-374168) DNA-PK (EMD Millipore NA57), Ku70 (Santa Cruz sc-5309), HA (Cell-Signaling Technology 2367), cyclin A (Millipore Sigma 06-138), cyclin E (Santa Cruz sc-377101), Rad54 (Santa Cruz sc-374598), and GFP (Santa Cruz sc-9996). Immunodetection was performed using LI-COR infrared imaging, or horse-radish peroxidase, via GeneSys G:Box F3 gel imaging system (Syngene).

Cell cycle synchronization

To isolate cells in G1, cells were treated with 8 μM Cdk1 inhibitor (RO −3306) for 20 hours, released into fresh media, and then collected 4 hours post release. To isolate cells in S phase, a double-aphidicolin block was used. Cells were treated with 10μM aphidicolin for 12 hours, released into fresh media for 8 hours, and then treated with aphidicolin for another 12 hours. Cells were released into fresh media and collected after 4 hours.

Immunofluorescence

U2OS cells grown on coverslips were washed twice in ice-cold phosphate-buffered saline (PBS) and pre-extracted three times for 10 minutes in 0.2% Triton X-100 and 2mM phenylmethylsulfonyl fluoride (PMSF) in PBS at 4°C. For visualization of DNA-PK, RNase A (0.3mg/mL) was added to our pre-extraction buffer (0.2% Triton-X) before fixation (Britton et al., 2013). Cells were washed with PBS and fixed in 4% formaldehyde in PBS for 10 minutes at room temperature. Cells were washed twice in room-temperature PBS and permeabilized in 0.5% Triton X-100 in PBS for 10 minutes at 4°C. For labeling with BrdU, cells were treated with 10 μM BrdU for a total of 3 hours before pre-extraction. Cells were treated with 2M HCl for 1 hour at room temperature, and then quenched using 0.5M sodium borate for 30 minutes. Cells were washed twice in room temperature PBST (0.1% Tween-20 in PBS) and blocked in 5% BSA in PBST for 1 hour at room temperature. Cells were then incubated with primary antibody overnight at 4°C. Antibodies used were γH2Ax (Millipore Sigma 05-636), γH2Ax (Abcam ab11174), $Sp1^{pS101}$ (Olofsson et al., 2007), 53BP1 (Millipore MAB3802), BRCA1 (Santa Cruz sc-642), BRCA1 (Novus Biologicals 6B4), DNA-PK (EMD Millipore NA57), Rad51 (Abcam ab1837), RIF1(Abcam ab13422), and BrdU (Abcam ab6326). Cells were washed in PBST three times followed by the addition of secondary antibodies, AlexaFluor 488—donkey anti-rabbit and AlexaFluor 594—donkey anti-mouse (Invitrogen; 1:1000 in 5% BSA), and AlexaFluor 405–donkey anti-rat for BrdU (Abcam), for 1 hour at room temperature. Cells were stained with 0.25 μg/mL DAPI (4',6-diamidino-2-phenylindole) in PBST for 5 minutes and then washed three times with PBST. Slides were mounted with VectaMount mounting medium (Vector Labs).

Fluorescence recovery after photobleaching

Cells transfected with GFP-53BP1 were treated with 10 μM BrdU for 24 hours. Fluorescence recovery after photobleaching was carried out on the Olympus Fluoview FV3000. Bleaching movies were acquired with photon collection in 1064 × 1064 pixels. Images during FRAP were acquired with the 405 nm laser line at a laser power of 80%, an EV gain of 500 and the PMT detection range was set to 500–540 nm for GFP acquisitions. One image was acquired prior to bleaching a circular area with using 80% laser power for one cycle, followed by 30 images to monitor the recovery. Signals were corrected for photobleaching using the unbleached area and then normalizing to the ratio between the average intensity of the prebleach images and the lowest post-bleach intensity. Averages ± standard deviation of SEM from 30 cells per condition were plotted.

Immunoprecipitation

The immunoprecipitation protocol was adapted from a previously described method (Kim et al., 1999). Cells were treated with 20 μM adriamycin for 1 hour. At the conclusion of treatment, cells were washed twice with PBS in ice and collected in 500 μL cold TGN buffer (50mM Tris [pH 7.5] 150mM NaCl, 1% Triton X-100, and protease and phosphatase inhibitors). Cells were disrupted 5 times with a tuberculin syringe and then sonicated twice for 30 s on/30 s off in bath sonicator (Diagenode Bioruptor Pico). Protein was quantified using BCA assay and 1.8 to 2.5 mg of protein lysate was used for each IP. A total of 10% of the lysate was saved for input. Cells were immunoprecipitated with pre-conjugated Flag-M2 beads (Sigma A2220) and incubated overnight at 4°C. Beads were washed twice with TGN buffer. Protein was eluted with 10X SDS sample buffer (500mM Tris [pH 6.8], 70% glycerol, and 25% [wt/vol] SDS. Precipitates were assessed by western blotting as described.

Chromatin immunoprecipitation

Briefly, $1.5x10^6$ U2OS cells were seeded on 15-cm dishes and infected 12 hours later with retrovirus expressing HA-ER-I-PpoI for 12 hours and then placed in phenol-free media supplemented with charcoal-stripped FBS. The ER fusion allows for nuclear localization of the enzyme after 4-OHT treatment of cells. Seventy-two hours post-infection, I-PpoI was induced by the addition of 8 μM 4-OHT (Sigma) to cell medium for 0.5, 1, 3, or 6 hours. For chromatin immmunoprecipitation, cells were crosslinked with 1% formaldehyde in PBS for 10 minutes. Reactions were quenched by the addition of 1.25M glycine for a final concentration of 125mM. Cells were then rinsed in ice-cold PBS and scraped and collected in PBS. Cell pellets were then lysed in 1mL of Nexon buffer (5mM PIPES [pH 8.0], 85mM KCl, and 0.5% [wt/vol] IGEPAL). Cells were disrupted once with a tuberculin syringe and then sonication 2x12 cycles for 30 s on/30 s off in a bath sonicator (Diagenode Biorupotor Pico). Cells were spun down and resuspended in shearing buffer (50mM Tris [pH 8.0], 10mM EDTA, and 0.1% [wt/vol] SDS). Chromatin was sheared by sonication for 8 cycles of 5 s on/30 s off. Lysate was diluted in dilution buffer (20mM Tris [pH 8.0], 1mM EDTA, 150mM NaCl, and 1% [wt/vol] Triton X-100), and protein was quantified in each treatment using a standard bicinchonic acid (BCA) assay, and samples were normalized to the same concentration. A total of 20% of the lysate was reserved, and genomic DNA was isolated as immunoprecipitation (Kang et al., 2012) input. The remaining lysate was then equally aliquoted and used for immunoprecipitation with Flag M2 pre-conjugated agarose beads, Nbs1 (Invitrogen MA-123265), GFP (Abcam ab290), BRCA1 (Novus Biologicals 6B4), γH2Ax (Millipore Sigma 05-636), or IgG (control, Abcam ab171870) antibodies. Antibodies other than Flag-M2 were preincubated with protein A/G agarose beads (Santa Cruz). All beads were pre-blocked with 1mg/mL low IgG bovine serum albumin (BSA) (Gemini Bio-Products) and 0.5mg/mL sheared salmon sperm DNA (ssDNA; Sigma) prior to IP. Immunoprecipitated DNA was isolated overnight, and beads were washed 3 times in low salt (20mM Tris [pH 8.0], 2mM EDTA, 150mM NaCl, 1% [wt/vol] Triton X-100, and 0.1% [wt/vol] SDS), high salt (20mM Tris [pH 8.0], 2mM EDTA, 500mM NaCl, 1% [wt/vol] Triton X-100, and 0.1% [wt/vol] SDS), and LiCl buffer (10mM Tris [pH 8.0], 1mM EDTA, 0.25M LiCl, 1% [wt/vol] NP-40, and 1% [wt/vol] sodium deoxycholate), respectively. DNA was purified using Chelex-100 resin as described previously (Nelson et al., 2006). Analysis of protein binding around the break site was assessed by SYBR green (Costa et al., 2019) quantitative PCR (qPCR) with previously published primers (Berkovich et al., 2007) by using a Bio-Rad CFX-96 real-time PCR detection system. Fold induction of binding was calculated using a modified $\Delta\Delta C_T$ method in which untreated and treated IP sample values are normalized to the differences in input DNA. Threshold cycle (C_T) values for control IPs and GAPDH control primers were used to set gates for background amplification.

Chromosome analysis

Cells were arrested in mitosis with 1 μg/mL of Nocodazole for 18h and harvested by shake-off, and centrifuged for 10 minutes at 1,000 RPM. Cells were swollen in 0.075 M KCl hypotonic solution at room temperature. Cells were fixed in 3:1 methanol:acetic acid solution at room temperature and dropped onto clean slides in a 37°C humidified chamber. Chromosomes were stained with DAPI.

DNA damage repair experiments

To measure DNA repair using the I-PpoI system, the chromatin immunoprecipitation protocol previously described was followed. Sample DNA concentrations were normalized, and analysis of DNA breaks was assessed by qPCR with previously published primers flanking the DNA break of the DAB1 gene (Berkovich et al., 2007). The percentage of damaged DNA was calculated using the $\Delta\Delta C_T$

method. The change in product from primers flanking the DAB1 break site was normalized to the change in product of primers that amplify an adjacent region 280 bp away from the cut site; the value calculated represents the fold change in product relative to control.

GFP-reporter EJ5 and DR-GFP U2OS cells (kind gift from Alexander Mazin, Drexel University College of Medicine, Pennsylvania, USA) were transduced with medium containing shRNA lentivirus. 48 hours later, cells were transduced with I-Sce1 exonuclease lentivirus. Seventy-two hours post-infection, analysis of DNA repair was assessed by flow cytometry (Guava easyCyte Flow Cytometer, Millipore) of GFP positive cells. DNA repair was calculated by first normalizing to background (without I-Sce1), and the value calculated represents the fold change in product to control. GFP-reporter EJ7 U2OS cells (kind gift from Jeremy Stark) were transduced with medium containing sgRNA lentivirus and/or pLZS-Sp1 constructs. Cells were then transfected with either GFP or sgRNA7a and sgRNA7b. Seventy-two hours post-infection, analysis of DNA repair was assessed by flow cytometry (Guava easyCyte Flow Cytometer, Millipore) of GFP positive cells. DNA repair was calculated by first normalizing to background (GFP only), and the value calculated represents the fold change in product to control.

Colony formation assay

UWB 1.289 and its derived cells lines were seeded onto a layer of 0.3% agar containing indicated doses of olaparib or ICRF-193 in six-well plates and overlayed with a 0.3% agar. The plates were incubated for 14 days, after which the cells were stained with p-iodonitrotetrazolium violet (INT) overnight and then photographed and counted.

QUANTIFICATION AND STATISTICAL ANALYSIS

Quantification of colocalization, foci number, and colony formation was performed using ImageJ. Data are represented as mean ± SEM and significant differences between groups was determined by two-tailed Student's t test, as specified in the figure legends. P values are indicated by nonsignificant ($p > 0.05$), *($p < 0.05$), **($p < 0.01$), or ***($p < 0.001$). Data without an explicit indication of statistical significance should be considered to have a P value greater than 0.05. All experiments were performed in triplicate, as specified in the figure legends. For immunofluorescence quantification, 30 cells were counted per experiment, also specified in the figure legends.